

AP-2 β IN THE DEVELOPMENT OF THE ANTERIOR SEGMENT OF THE EYE

ANTERIOR SEGMENT DYSGENESIS AND GLAUCOMATOUS FEATURES
OBSERVED FOLLOWING CONDITIONAL DELETION OF AP-2 β IN THE NEURAL
CREST CELL POPULATION

By

VANESSA MARTINO, B.SC. (HONOURS)

A Thesis

Submitted to the School of Graduate Studies

In Partial Fulfillment of the Requirements

For the Degree

Master of Science

McMaster University

©Copyright by Vanessa Martino, August 2015

MASTER OF SCIENCE (2015)

McMaster University

(Medical Sciences)

Hamilton, Ontario

TITLE: Anterior Segment Dysgenesis and Glaucomatous Features
Observed following Conditional Deletion of AP-2 β in the
Neural Crest Cell Population

AUTHOR: Vanessa Martino, B.Sc. (Honours) (University of Guelph)

SUPERVISOR: Dr. Judith A. West-Mays

NUMBER OF PAGES: ix, 94

ABSTRACT

Glaucoma is a heterogeneous group of diseases that is currently considered to be the leading cause of irreversible blindness worldwide. Of the identified risk factors, elevated intraocular pressure remains the only modifiable risk factor that can be targeted clinically. Ocular hypertension is often a result of dysregulation of aqueous humour fluid dynamics in the anterior eye segment.

Aqueous humour drainage is regulated by structures located in the anterior chamber of the eye. In some circumstances dysregulation occurs due to developmental abnormalities of these structures. The malformation of structures in the anterior segment is thought to be due to a defect in the differentiation and/or migration of the periocular mesenchyme during development. Unique to vertebrates, the neural crest cell (NCC) population contributes to the periocular mesenchyme and is instrumental to the proper development of structures in the anterior segment.

For many years our laboratory has examined the role of the Activating Protein-2 (AP-2) transcription factors that are expressed in the neural crest and vital during the development of the eye. The purpose of this research project is to investigate the role of AP-2 β in the NCC population during the development of the anterior segment of the eye.

Conditional deletion of AP-2 β expression in the NCC population demonstrated that mutants have dysgenesis of structures in the anterior segment including defects of the corneal endothelium, corneal stroma, ciliary body and a closed iridocorneal angle. Loss of retinal ganglion cells and their axons was also observed, likely due to the disruption of aqueous outflow, suggesting the development of glaucoma.

The data generated from this research project will be critical in elucidating the role of AP-2 β in the genetic cascade dictating the development of the anterior eye segment in addition to providing scientific research with a novel model of glaucomatous optic neuropathy.

ACKNOWLEDGEMENTS

To my supervisor, Dr. Judy West-Mays, I would like to take this opportunity to sincerely thank you for all your support, advice and mentorship over the past two years. Your enthusiasm for research and graduate work as well as your advocacy for your students is so admirable and appreciated. You are a true role model and inspiration for all women in science. I have been truly fortunate to have had you as my supervisor, and I cannot thank you enough for all the opportunities you have granted me, the confidence you have instilled in me and all that you have taught me.

I would also like to thank my committee members, Dr. Ball and Dr. Bridgewater. Dr. Ball, thank you for all your expertise, guidance and advice - your enthusiasm for science is infectious and your assistance with my project was invaluable. Dr. Bridgewater, thank you for your guidance and words of encouragement throughout my graduate studies, it was greatly appreciated. Also thank you to Dr. Doering, not only for your support and advice but for also allowing me to use your microscope.

To the wonderful Paula Deschamps, thank you for all the work you do for us in the lab, it does not go unnoticed. I am truly grateful I have had the pleasure of working alongside you, and I know I'm leaving my furry little friends in good hands. Also, to Janis MacDonald, thank you for taking such good care of my little mutants. You have my deep admiration for your dedication to your work and your charges. To my past lab mates, Mizna Zaveri, Anuja Siwakoti, Dr. Madhuj Gupta and Dr. Christine Kerr, thank you for welcoming me into the lab and for your mentorship, advice and support as I began to navigate the waters of graduate school - I am deeply appreciative. To the current members of the West-Mays lab, future Drs. Anna Korol and Scott Bowman, Dr. Aftab Taiyab and fellow graduate student Emily Anne Hicks, it has been my privilege to have worked alongside each of you. I sincerely thank you all for your patience with my endless questions, your assistance with all matters related to science and for making my graduate experience unforgettable. As I said when I began my Masters, coming into work every morning is such a pleasure because I have the opportunity to be a part of such a lovely group of people that I consider not only colleagues but also friends. I wish you all nothing but the best.

I would also like to thank the members of the Ball and Doering labs, Tom Sabljic, Connie Cheng, Mary Sourial, Jessica Wallingford and Angela Scott. In particular, to Tom and Connie, thank you both for your help, support and advice both at the bench and outside of the lab.

Lastly, I would like to express my heartfelt gratitude to my parents and brother. All my achievements are directly attributable to your constant love, unwavering support and endless encouragement, for which I will always be eternally grateful.

TABLE OF CONTENTS

ABSTRACT	iii
ACKNOWLEDGEMENTS	v
LIST OF TABLES & FIGURES	viii
LIST OF ABBREVIATIONS	ix
CHAPTER ONE	1
GENERAL INTRODUCTION	1
1.1 Glaucoma	2
1.1.1 Epidemiology	2
1.1.2 Relationship between increased IOP and Glaucoma	3
1.1.3 Animal Models of Glaucoma	5
1.2 Anterior Segment Dysgenesis	7
1.3 Development of the Anterior Segment of the Eye	9
1.4 Key Genes expressed in the POM involved in the Development of the Anterior Segment	13
1.5 Activating Protein-2 Transcription Factors	15
CHAPTER TWO	22
RATIONALE, MAIN HYPOTHESIS & RESEARCH AIMS	22
2.1 Rationale for the study	23
2.2 Main Hypothesis	24
2.3 Research Aims	24
CHAPTER THREE	27
EXPERIMENTAL DESIGN	27
3.1 Animal Husbandry	28
3.2 Generation of AP-2 β NCC KO Mutants	28
3.3 Histology	29
3.4 Immunofluorescence	29
3.5 Anterior Segment Imaging with the Phoenix Micron IV Imaging Microscope and OCT attachment	30
3.6 IOP Measurements	31
3.7 RGC tracing with Neurobiotin	32
3.8 Electron Microscopy	32
3.9 Quantification and Statistical Analysis	33
CHAPTER FOUR	35
RESULTS	35
4.1 Generation of AP-2 β NCC KO mutants	36
4.2 Histological examinations of AP-2 β NCC KO embryonic and adult mutants	37
4.3 Increased IOP in AP-2 β NCC KO mutants relative to wildtype littermates	40
4.4 Decreased retinal thickness in P42 AP-2 β NCC KO mutants	40
4.5 Loss of RGCs in two-month old AP-2 β NCC KO mutant retinae relative to wildtype littermates	41
4.6 Loss of retinal ganglion cell axons in ONs	43
4.7 Increased glial reactivity of the retina	44

CHAPTER FIVE	46
DISCUSSION, FUTURE DIRECTIONS & CONCLUSION	46
DISCUSSION	47
5.1 AP-2 β expression in NCCs and the development of the anterior eye segment	48
5.2 AP-2 β NCC KO mutants as a model of glaucoma	52
FUTURE DIRECTIONS AND CONCLUSION	56
REFERENCES	59
FIGURES	70

LIST OF TABLES AND FIGURES

Table 1. PCR protocols	34
Figure 1. General Anatomy of the Eye	71, 72
Figure 2. Schematic depicting theories behind the relationship between increased IOP and the development of glaucoma	73
Figure 3. Vertebrate eye development and tissue derivations	74
Figure 4. Migration of the POM in the mouse eye and development of the anterior segment	75,76
Figure 5. The expression of AP-2 α and AP-2 β in an E15.5 murine eye	77
Figure 6. Generation of AP-2 β NCC KO mutants	78
Figure 7. PCR results	79
Figure 8. Conditional deletion of AP-2 β in the NCC population in AP-2 β NCC KO mutant embryos	80
Figure 9. Early eye development of AP-2 β NCC KO mutants relative to wildtype littermates	81
Figure 10. Abnormal development of the anterior segment in P42 AP-2 β NCC KO mutants	82
Figure 11. OCT images displaying a closed iridocorneal angle of P42 AP-2 β NCC KO mutants	83
Figure 12. Missing corneal endothelium and anterior subcapsular cataracts in P42 AP-2 β NCC KO mutants	84
Figure 13. Missing corneal endothelium in E18.5 AP-2 β NCC KO mutant embryos	85
Figure 14. Corneal neovascularization in P42 AP-2 β NCC KO mutants	86
Figure 15. A comparison of intraocular pressure (IOP) between three-month-old AP-2 β NCC KO mutants and their wildtype littermates	87
Figure 16. Decreased overall retinal and IPL thickness in P42 AP-2 β NCC KO mutants	88
Figure 17. Loss of Brn3a expression in AP-2 β NCC KO mutants	89
Figure 18. Labeling of RGCs and nuclei in two-month-old AP-2 β NCC KO mutants	90
Figure 19. Decreased number of RGCs, total nuclei and dACs in two-month-old AP-2 β NCC KO mutants	91
Figure 20. Transmission electron microscopy of two-month-old AP-2 β NCC KO mutant ONs and their wildtype littermates	92
Figure 21. Decreased cross-sectional area of two-month-old AP-2 β NCC KO mutant optic nerves	93
Figure 22. Increased retinal glial reactivity in mutant retinas	94

LIST OF ABBREVIATIONS

AP-2	Activating Protein-2	NCC	Neural crest cell
ASD	Anterior Segment Dysgenesis	NFL	Nerve fiber layer
ASD ^{nc}	neural-crest ASD	NR	Neural retina
ASD ^{non-nc}	non-neural crest ASD	ON	Optic nerve
BOFS	Branchio-Oculo-Facial Syndrome	ONH	Optic nerve head
E	Embryonic Day	OPL	Outer plexiform layer
GCL	Ganglion cell layer	P	Post-natal day
H&E	Hematoxylin & Eosin	PACG	Primary angle closure glaucoma
INL	Inner nuclear layer	PCR	Polymerase chain reaction
IOP	Intraocular Pressure	POAG	Primary open angle glaucoma
IPL	Inner plexiform layer	POM	Periocular mesenchyme
KO	Knockout	RGC	Retinal ganglion cell
NB	Neurobiotin	RPE	Retinal Pigmented Epithelium
		SD	Standard Deviation

CHAPTER ONE
GENERAL INTRODUCTION

1.1 Glaucoma

Glaucoma is a multifactorial disease process that is characterized by a loss of retinal ganglion cells (RGCs), excavation of the optic nerve head (ONH) and defects of specific visual fields (Ritch, R. et al., 1996). A variety of risk factors for glaucoma exist including age, race, genetics, family history, comorbidities, corneal thickness and high intraocular pressure (IOP) (Boland and Quigley 2007, Coleman and Miglior 2008). Increased IOP stands as the only modifiable risk factor of glaucoma and the only clinically accepted target for therapeutic strategy (Chang and Goldberg 2012, Kolko 2015). However, it should be noted that elevated IOP does not necessarily result in optic nerve (ON) and subsequent retinal damage, and glaucomatous damage can still occur despite normal IOP levels (Araie, Sekine et al. 1994).

1.1.1 Epidemiology

Glaucoma is the current leading cause of irreversible blindness worldwide, and due to the rapidly aging population is predicted to affect over 70.6 million people by 2020 and 111.8 million people by 2040 globally with a disproportionate prevalence seen in Asian and African countries (Quigley and Broman 2006, Tham, Li et al. 2014). Glaucoma is often classified into two types, primary open angle glaucoma (POAG) and primary angle closure glaucoma (PACG). POAG is more commonly seen in patients worldwide accounting for 74% of glaucoma cases reported (Quigley and Broman 2006). In the United States, prevalence of POAG in people of African American and Hispanic descent is more frequently observed with a 3-fold and 3-4-fold increase respectively when

compared to white subjects (Friedman, Wolfs et al. 2004, Varma, Ying-Lai et al. 2004). Comparatively, Asian populations account for the majority of glaucoma cases worldwide with 47%, and the large majority of PACG with 87% of patients being of Asian descent (Quigley and Broman 2006). The economic burden in Canada of vision loss related health care costs is substantial costing Canadians \$3.5 billion in 2007, accounting for 2.2% of all health care expenditures. Glaucoma accounts for \$549 million of this cost, and 10.2% of total nervous drug expenditure for total nervous system and sense organ disorders (CNIB 2011).

1.1.2 Relationship between increased IOP and Glaucoma

As previously mentioned, IOP is currently the only clinically modifiable risk factor for glaucoma. In order to appreciate the relationship that exists between IOP and glaucoma an understanding of the anatomy of the eye and the aqueous outflow pathway must be established (Figure 1A-B). In a normal eye, aqueous humour produced by the ciliary body will travel between the lens and the posterior iris, and exit through the pupil to enter the anterior chamber. It will then travel towards the iridocorneal angle (formed at the junction of the cornea and iris) where drainage structures, the trabecular meshwork and Schlemm's canal, are located to allow for the fluid to exit the eye. In the case where aqueous humour is unable to exit through the drainage structures there will be an increase in the pressure within the anterior chamber that will translate to an increase in fluid pressure of the eye, known as IOP.

The factors that lead to damage of the ON and loss of RGCs still remain unknown, but a variety of theories exist in an attempt to provide an explanation. One theory proposed by Müller in 1858 suggested that the increase in IOP induced mechanical trauma at the ONH caused neuronal loss; von Jaeger (1858) believed that glaucomatous damage was a result of compromised vasculature at the ONH (Dreyer and Lipton 1999). In the late twentieth century it was shown that axoplasmic transport at the lamina cribrosa of the ONH was impeded when IOP was elevated, thereby preventing trophic factors from reaching the RGCs, which would in turn stimulate programmed cell death (Lampert, Vogel et al. 1968, Anderson and Hendrickson 1974, Quigley and Anderson 1976). Further evidence has supported that anterograde and retrograde export is disturbed at the ONH when IOP has been increased, and the blockade is reversed once the IOP has normalized (Minckler, Bunt et al. 1977). Another study displayed impediment of retrograde transport of neurotrophin BDNF (Brain-derived neurotrophic factor) in acute and chronic animal models of increased IOP, supporting the role of neurotrophin deprivation in RGC death and glaucomatous optic neuropathy (Pease, McKinnon et al. 2000). Increased IOP has also been shown to cause glial activation of astrocytes and microglia that have both neuroprotective and neurodegenerative roles in response to CNS injury with the release of cytotoxic substances (Neufeld, Hernandez et al. 1997). Metabolic and endoplasmic reticulum stress have also been seen to increase at the ONH alongside increase of IOP, potentially contributing to the death of RGCs (Shimazawa, Inokuchi et al. 2007, Ju, Kim et al. 2008). Therefore, the evidence would support that an

increase in IOP could cause damage at the ONH leading to the loss of retinal ganglion cells and glaucomatous optic neuropathy (Figure 2).

1.1.3 Animal Models of Glaucoma

In order to further understanding of the disease processes of glaucoma the development of animal models is essential to advancement in this field. There are a variety of animal models utilized from a range of species including monkeys, rabbits, dogs, cats and rodents. Although many exist, due to the complexity of the disease an ideal model of glaucoma that completely mimics the human condition has yet to be created. For the purposes of this work we will be focusing on mouse animal models that can be categorized into inducible models and spontaneous/genetic models. Mice are an attractive model system to utilize for a number of reasons including the high degree of conservation between the human and mouse genome, the ease of breeding so that high cohorts can be obtained relatively inexpensively and, perhaps most importantly, the opportunity for genetic manipulation of the mouse genome allowing for the study of complex genetic interactions of critical genes and biochemical pathways. Inducible models of glaucoma in mice are often obtained by creating an obstruction of the aqueous outflow pathways leading to an increase in IOP. Methods to achieve this, adapted from successful rat models, include episcleral vein occlusion (Ruiz-Ederra and Verkman 2006), laser photocoagulation of episcleral veins (Aihara, Lindsey et al. 2003), injection of hypertonic saline into episcleral veins resulting in sclerosis (McKinnon, Schlamp et al. 2009) and injection of microbeads into the anterior chamber (Sappington, Carlson et al. 2010). An

advantage of inducible models of glaucoma is the ability to use the contralateral eye as a control, however the elevation in IOP is often transient with the procedure needing to be repeated if a long-term study is designed.

Spontaneous or genetic mouse models of glaucoma have also been developed to further research in the field. Perhaps the most well characterized is the inbred DBA/2J strain that developed spontaneous mutations in two separate genes encoding melanosomal proteins (Anderson, Smith et al. 2002). Mice of the DBA/2J inbred line that are homozygous for a recessive mutant allele of *Tyrp1b* and a premature stop codon in the *Gpnmb* gene will develop characterized iris stromal atrophy and pigment dispersion pathology of the anterior chamber, which will accumulate in drainage structures and cause a blockage leading to an elevation of IOP (John, Smith et al. 1998). The DBA/2J strain develops iris atrophy by 6-8 months of age and registers a significant elevation in IOP between 8-13 months of age. In addition, they often have variable phenotypes necessitating a large cohort of animals to be studied (Libby, Anderson et al. 2005). Other transgenic mouse models that exist include mice with a targeted mutation in the $\alpha 1$ subunit of collagen type I (*Col $\alpha 1$ ^{+/+}*) that disrupts aqueous humour outflow due to an accumulation of collagen type I (Aihara, Lindsey et al. 2003), and mice with mutations in myocilin (*Tyr437His*) which is secreted in the trabecular meshwork (Senatorov, Malyukova et al. 2006). Both of these models produce a modest elevation in IOP with only 28.7% and 20% RGC loss seen respectively at over 18 months of age.

Another avenue for glaucoma models include mouse models with defects in the development of the anterior chamber of the eye and its structures which lead to elevations

of IOP and loss of RGCs. Mice with mutations of *Sh3pxd2b* (*nee* mice) experience abnormalities in the development of the anterior chamber that lead to a drastic increase in IOP and early degeneration of the ONH relative to the previous models mentioned (Mao, Hedberg-Buenz et al. 2011). Abnormalities such as those found in the *nee* mice are known as anterior segment dysgenesis and this is discussed in the following section.

1.2 Anterior Segment Dysgenesis

Anterior segment dysgenesis (ASD) is a spectrum of disorders that involves developmental malformations of tissues found in the anterior segment of the eye including the cornea, iris, lens and drainage structures. A primary defect in the differentiation and/or migration of neural crest cells (NCCs) that contribute to the development of these structures is suspected to be responsible (Kupfer and Kaiser-Kupfer 1978, Kupfer and Kaiser-Kupfer 1979). ASDs are associated with a variety of phenotypes including cloudy corneas, misshapen or displaced pupils and iridocorneal attachments, and differences in expressivity and penetrance of phenotypes are also apparent suggesting a complex etiology. A variety of genes are linked to ASD in patients and currently nine different genes (*PAX6*, *PITX2*, *PITX3*, *FOXC1*, *FOXE3*, *EYA1*, *CYP11B1*, *LMX1B* and *MAF*) have been associated with ASD or glaucoma in humans, with evidence of many other potential candidate genes (Gould and John 2002). Interestingly, mutation of a specific gene does not always result in consistent phenotypes, and evidence suggests that the type of mutation could influence the severity of ASD that arises. An example of this would be mutations in *PITX2*, a paired-like homeodomain transcription factor, that

present with a variety of phenotypes including, Rieger syndrome, iris hypoplasia and iridogoniodysgenesis (Perveen, Lloyd et al. 2000). However, it has also been observed that patients with the same mutation of a specific gene present with different phenotypes, signifying that other factors such as environmental, lifestyle and genetic influences could be contributing to this multifactorial developmental disorder (Mears, Mirzayans et al. 1996). The ability to eliminate and control for genetic and environmental factors would facilitate the study of this complex disease process, pointing to the effectiveness of inbred mouse models of ASD.

ASDs can be divided into two sub-groups, neural-crest ASDs (ASD^{nc}) and non-neural crest ASDs (ASD^{non-nc}). ASD^{nc} encompasses ASDs in which the structures that are malformed are of neural crest derivation (i.e. corneal stroma and endothelium, ciliary body stroma and muscle, anterior iris stroma, iridocorneal angle, drainage structures, etc.) while ASD^{non-nc} involves abnormalities in anterior structures derived from non-neural crest origin (i.e. corneal epithelium, lens, pigmented ciliary body and iris epithelium, etc.) (Idrees, Vaideanu et al. 2006). ASDs with abnormalities affecting the aqueous outflow pathway (whether anatomically or functionally), more commonly seen in ASD^{nc} , often result in an increase in intraocular pressure (IOP), creating an environment favourable to the development of glaucoma (Shields 1987). Further understanding of the development of the eye and its anterior chamber, and the genes that are involved, will assist in further elucidating the causes and consequences of anterior segment dysgenesis.

1.3 Development of the Anterior Segment of the Eye

The eye has long been studied as a model of embryonic induction and differentiation. The bilateral evagination of the diencephalon, a derivative of the embryonic neural tube, marks the first morphological presence of the vertebrate eye known as the optic pit (Chow and Lang 2001). The optic pit will evaginate further to form the optic vesicle, which will displace mesenchymal cells as it extends toward the overlying non-neural surface ectoderm (Figure 3A). Once the tissues are in close vicinity the neuroepithelium will send inductive signals instructing the head ectoderm to thicken and form the lens placode at embryonic day 9.5 (E9.5) (Pei and Rhodin 1970, Graw 1996). Both the optic vesicle and lens placode will then invaginate to form the double-layered optic cup and lens vesicle respectively (Chow and Lang 2001) (Figure 3B-C). The outer layer of the optic cup will differentiate to become the retinal pigmented epithelium (RPE) and the inner layer of the optic cup will constitute the neural retina (NR) (Figure 3C) (Graw 1996). The lens vesicle, which has been pinched off from the overlying surface ectoderm, will differentiate into a transparent lens that will allow for the passage of light to reach the retina. The cornea and anterior eye segment will develop due to a highly coordinated, multi-step process involving the overlying surface ectoderm and migrating NCCs (Graw 1996, Chow and Lang 2001, Gilbert 2006)(Figure 3C).

The anterior segment of the eye includes the following structures: the cornea, lens, iris, ciliary body, trabecular meshwork and Schlemm's canal. The cornea is a highly specialized transparent tissue that, alongside the lens, is responsible for the refraction of light. Both the cornea and lens have angiogenic privilege, that is the absence of blood and

lymphatic vessels, which is necessary for optimal transparency and normal vision (Ellenberg, Azar et al. 2010). The iris is responsible for regulating the amount of light that enters the eye by controlling the size and diameter of the pupil. Aqueous humour, a clear fluid, is secreted by the ciliary body to provide nutrition to the avascular cornea and lens. The induction and differentiation of surface ectoderm, neural ectoderm and periocular mesenchyme (POM) are responsible for the development of these structures (Gould, Smith et al. 2004). The surface ectoderm will give rise to the corneal epithelium and lens, and the neural ectoderm will form the retina and epithelia of the iris and ciliary body. The POM, which consists of cranial NCCs and mesoderm, will derive the corneal stroma, corneal endothelium, iris stroma, ciliary body muscle, ciliary body stroma and trabecular meshwork (Figure 3D) (Gould, Smith et al. 2004, Gage, Rhoades et al. 2005).

Unique to vertebrates, NCCs are a transient, migratory and multipotent cell population that gives rise to a variety of different cell types throughout the body. In the beginning phase of neural development the ectodermal (outer) layer of the embryo will give rise to neural tissue during a process known as neural induction. As a result, the ectoderm will be divided into three regions, the neural plate/ectoderm (the future CNS), the non-neural ectoderm (the future epidermis) and the cells that lie at this border between the two regions, known as the neural fold, which will mostly give rise to NCCs. Neurulation will then occur as the neural plate borders join each other to form the neural tube, while the NCCs delaminate from the neural folds (Gammill and Bronner-Fraser 2003). Until migration occurs the NCCs are not yet a defined cell population and are considered to be “pre-migratory” as previous studies have demonstrated that cells within

the neural folds are still able to contribute to the epidermis and neural tube in addition to the NCC population (Serbedzija, Bronner-Fraser et al. 1994). They will then undergo an epithelial-mesenchymal transition and migrate via defined predetermined pathways within the embryo. The NCC population can be categorized into three different groups, (1) cardiac NCCs which will contribute to the thyroid, parathyroid, thymus and heart outflow tract, (2) trunk NCCs which will assist in the formation of the dorsal root ganglia, enteric nervous system, melanocytes and adrenal gland, and (3) cranial NCCs, which will give rise to neurons and glia of the cranial ganglia and melanocytes within the head, craniofacial skeleton and connective tissue (Brewer, Feng et al. 2004). As previously mentioned, cranial NCCs will contribute, along with the mesoderm, to the POM in the vertebrate eye.

Once the lens vesicle has pinched off at E10.5, the POM will begin to infiltrate the space between the lens vesicle and the overlying surface ectoderm (Figure 4A) (Pei and Rhodin 1970). By E12.5 four to seven layers of mesenchymal cells will be present and the first structures of the cornea will begin to develop (Figure 4B) (Haustein 1983). The cells closest to the lens will flatten and connect with adjacent cells through junctional complexes as a monolayer to form the corneal endothelium by E14.5-15.5 (Reneker, Silversides et al. 2000). Meanwhile the surface ectoderm will give rise to the corneal epithelium which originates as a two layered structure that will later expand into a 4 to 5 cell layer stratified squamous non-keratinized epithelium (Pei and Rhodin 1971). The mesenchymal cells between the corneal endothelium and epithelium will differentiate into the corneal stroma, which will be responsible for maintaining corneal transparency

through the synthesis of a highly specialized extracellular matrix (Figure 4C) (Haustein 1983).

As the corneal endothelium differentiates, the anterior peripheral edge of the optic cup will expand into the space between the posterior cornea and anterior lens to later give rise to the iris and ciliary body (Pei and Rhodin 1970). A second wave of mesenchymal cells will migrate to the area of the presumptive iridocorneal angle then along the epithelia layers of the iris and ciliary body where they will finally differentiate into the stroma of both structures (Cvekl and Tamm 2004). By E16.5 the iris stroma is no longer connected to the cornea and the anterior chamber is formed (Figure 4C) (Smith, Zabaleta et al. 2001). As the iris begins to elongate (E17.5-19.5) the iridocorneal angle will be occupied with a dense mass of cells that will give rise to the tissues of the aqueous outflow pathway (i.e. the trabecular meshwork and Schlemm's canal) (Figure 4D box). The majority of development of the trabecular meshwork and Schlemm's canal will occur post-natally, reaching near completion by post-natal day 42 (P42) (Smith, Zabaleta et al. 2001). The mesenchymal cells will flatten and elongate while extracellular fibers will fill the small spaces that are created as the cells begin to separate. The extracellular fibers will become covered in endothelial-like cells and organize into beams or lamellae, ultimately giving rise to the trabecular meshwork which consists of trabecular beams that are separated to allow aqueous humour to flow through the intertrabecular spaces to Schlemm's canal (Cvekl and Tamm 2004). Schlemm's canal contacts the outer portion of the trabecular meshwork and is united with the scleral vessels. Between P10-14 endothelial cells line a small lumen that will become Schlemm's canal (Smith, Zabaleta et

al. 2001). Aqueous humour will pass through the endothelial wall into drainage structures known as giant vacuoles and ultimately into the venous system (Cvekl and Tamm 2004). As previously mentioned, abnormal development of these drainage structures can potentially lead to an elevation in IOP and subsequently glaucoma (Gould, Smith et al. 2004).

1.4 Key genes expressed in the POM involved in the Development of the Anterior Segment

While the genetic cascade that governs the development of structures of the anterior eye still remains to be elucidated, some of the genes involved have been identified. As explained above, the POM is essential for proper formation of the anterior segment of the eye, and a variety transcription factors expressed in the POM have been implicated in incidences of ASD and glaucoma.

Transcription factors FOXC1 and FOXC2 share near identical DNA binding domains and similar expression patterns in the POM. Mice that are homozygous null for *Foxc1* (*Foxc1*^{-/-}) exhibit severe ASD with no corneal endothelial differentiation, a disorganized corneal stroma, a thickened corneal epithelium and failure of separation of the cornea and lens that consequently causes no anterior chamber to form (Kidson, Kume et al. 1999). Due to the extensive congenital abnormalities that arise from the mutation these mice die at birth precluding further analysis of anterior segment development (Kume, Deng et al. 1998). Mice heterozygous for this mutation (*Foxc1*^{+/-}) do survive past birth and present with a milder form of ASD with malformation of the iris, cloudy

corneas, closed angle phenotypes and deformities of drainage structures of the iridocorneal angle (Smith, Zabaleta et al. 2000). A spectrum of phenotypes of ASD and glaucoma manifest in patients with mutations in *FOXC1*. Mice that have mutations of *Foxc2* experience similar ocular phenotypes suggesting overlapping function between the two family members in development of the eye, however no analogous human condition for *FOXC2* mutation has yet been identified (Smith, Zabaleta et al. 2000).

Also expressed in the POM is paired-like homeodomain transcription factor PITX2 beginning at E9.5. Expression of *Pitx2* continues in the presumptive corneal stroma, iris and iridocorneal angle and the pattern of expression is similar to that of *Foxc1* and *Foxc2* (Gage, Suh et al. 1999). Mutant mice homozygous null for *Pitx2* (*Pitx2*^{-/-}), which are not viable past E15.5, do not develop a corneal endothelium or anterior chamber, and have a thickened, undifferentiated corneal epithelium (Gage, Suh et al. 1999, Lu, Pressman et al. 1999). Both *FOXC1* and *PITX2* have been implicated in patients with Axenfeld-Rieger syndrome, an autosomal dominant syndrome that presents with a range of congenital abnormalities of structures in the anterior segment of the eye (Tumer and Bach-Holm 2009). These genes are also found to be dosage responsive, and a disease causative state can be triggered with changes in levels of functional protein during development.

LMX1B is another transcription factor expressed in the POM and presumptive cornea beginning at E10.5. Mutant mice homozygous negative for *Lmx1b* (*Lmx1b*^{-/-}) have a variety of ocular defects including smaller eyes, hypoplasia of the iris and ciliary body, and the keratocytes of the corneal stroma are less densely packed (Pressman, Chen et al.

2000). Unfortunately, these mutants are also not viable past birth impeding the analysis of post-natal anterior segment development. In humans, mutations in *LMX1B* has been linked to nail-patella syndrome which has been associated with glaucoma (Lichter, Richards et al. 1997, Knoers, Bongers et al. 2000).

These are only a few of the genes implicated in ASD and glaucoma in humans and there likely are many more candidate genes to be identified in order to gain a better understanding of the genetic cascade that regulates the development of the POM and anterior eye.

1.5 Activating Protein-2 Transcription Factors

The Activating Protein-2 (AP-2) transcription factors are a family of retinoic acid responsive proteins, whose involvement is vital during the development of multiple tissues, including ocular morphogenesis. There are five known AP-2 transcription factors that exist in both mice and humans, AP-2 α , AP-2 β , AP-2 γ , AP-2 δ and AP-2 ϵ , transcribed from genes labeled *tcfap2 α - ϵ* in mice and *TFAP2 α - ϵ* in humans. Orthologs of some of these proteins, sharing an amino acid similarity between 60-99%, can also be found in fish and frogs (Eckert, Buhl et al. 2005). The proteins form both homo- and heterodimers, which is facilitated by their characterized c-terminal helix-span-helix dimerization motif followed by a central basic region that is highly conserved throughout the family, and also assumes responsibility for DNA binding. Transactivation occurs at the less conserved proline- and glutamine-rich amino terminus (Eckert, Buhl et al. 2005). The palindromic consensus sequence 5'-GCCNNNGGC-3' has been determined to be the DNA binding

site for the AP-2 transcription factor family, however additional binding motifs also exist suggesting that an array of G/C-rich sequences with variable affinities may act as binding sites for AP-2 (Mohibullah, Donner et al. 1999). The AP-2 transcription factor family has been found to have a regulatory role in cell cycle control, differentiation and apoptosis through various mechanisms (Hilger-Eversheim, Moser et al. 2000).

The expression patterns of the *Tcfap2* family are both unique and overlapping with initial expression first detected in pre-migratory NCC population, continuing expression during migration and in its derivatives including cranial and dorsal root ganglia, facial structures and pigment cells. Expression also occurs in epidermal tissues and its derivatives, structures of the central and peripheral nervous system, development of renal and urogenital tissues, and in proliferating mesenchymal cells in developing limb buds (Mitchell, Timmons et al. 1991). As such, the proper function of the AP-2 transcription factor family is critical for vertebrate embryogenesis to occur normally, as AP-2 α knockout (KO) mice (*Tcfap2 α ^{-/-}*) exhibit severe congenital deformities and die perinatally (Schorle, Meier et al. 1996, Zhang, Hagopian-Donaldson et al. 1996, Moser, Pscherer et al. 1997, Hilger-Eversheim, Moser et al. 2000). Mice that are germline *Tcfap2 β ^{-/-}* exhibit increased apoptosis of kidney epithelial cells as well as the development of renal cysts resulting in death shortly after birth (Moser, Pscherer et al. 1997).

Our laboratory has an extensive history studying the importance of AP-2 transcription factors and has shown that *Tcfap2* gene expression plays an important role in ocular genesis. Mice that are *Tcfap2 α ^{-/-}* germline KO (herein referred to as AP-2 α ^{-/-})

exhibit mutant ocular phenotypes including abnormalities of the optic cup, failed or defective lens induction and absent cornea and eyelids (West-Mays, Zhang et al. 1999). Defects of the presumptive retina (optic cup) arose by E12.5 in which the dorsal side of the optic cup had been replaced with a duplicated retina and there was an absence of the RPE. The inner plexiform and ganglion cell layers were also absent in older germline mutants (West-Mays, Zhang et al. 1999). Due to the lethality of AP-2 α ^{-/-} phenotype (Schorle, Meier et al. 1996, Zhang, Hagopian-Donaldson et al. 1996) ocular development can only be observed until birth, necessitating a need for conditional knockouts in which AP-2 α would be deleted from specific tissues. Utilizing Cre-loxP technology our lab has generated mutants that have AP-2 α conditionally deleted from the developing lens placode, referred to as Le-AP-2 α mutants. These mutants exhibited defective corneal and lens phenotypes, similar to what was seen in the germline AP-2 α ^{-/-} mutants, confirming a cell autonomous role for AP-2 α in lens-placode derived tissues. However, the optic cup defects previously seen in the germline mutants were not observed in the conditional mutants (Pontoriero, Deschamps et al. 2008).

Once again employing Cre-loxP technology, mutants in which AP-2 α was conditionally deleted from the presumptive retina (labeled Ret-AP-2 α) were created to observe if AP-2 α had a cell autonomous role in the retina. Surprisingly, there was no retinal phenotypic variance between the conditional mutants and wildtype littermates, suggesting a non-cell-autonomous role for AP-2 α (Bassett, Pontoriero et al. 2007). It was then hypothesized that perhaps the family member AP-2 β was playing a compensatory role, supported by previous studies which reported a high degree of conservation among

the intron-exon structure and protein sequences of AP-2 α and AP-2 β , suggesting a common ancestral gene origin (Moser, Imhof et al. 1995). These two transcription factors are also able to bind as heterodimers in vitro, bind the same sites on a given promoter, as well as regulate the transcription of the same genes (Moser, Imhof et al. 1995, Boshier, Totty et al. 1996). They also display near identical expression patterns in the early embryo (Moser, Ruschoff et al. 1997). In older embryos expression of *Tcfap2 β* was found to be similar to that of *Tcfap2 α* , with both being expressed in the inner nuclear layer (INL) of the developing retina, and both being co-expressed in a subset of amacrine cells in the adult mammalian retina. Furthermore, expression of *Tcfap2 β* was strong in the developing INL of Re-AP-2 α mutants, proposing functionally redundant roles of the two AP-2 family members in the developing vertebrate retina (Bassett, Pontoriero et al. 2007).

To address the possible overlapping roles of AP-2 α and AP-2 β in retinogenesis the Re-AP-2 α mutants were then crossed onto a global *Tcfap2 β* ^{-/-} background thereby creating a model in which AP-2 α was conditionally deleted from the retina and AP-2 β was deleted from all tissues (AP2 α ^{lacZki/lox}/ AP-2 β ^{-/-}). This allowed for examination of retinogenesis up until death at P0 (Bassett, Korol et al. 2012), since the global *Tcfap2 β* ^{-/-} deletion results in kidney failure and lethality. The Ret-AP-2 α /AP-2 β ^{-/-} mutant retinas displayed irregular staining of amacrine cells and loss of horizontal cells, neither of which was seen upon individual deletion of AP-2 α or AP-2 β (Bassett, Korol et al. 2012), demonstrating the overlapping role of AP-2 α and AP-2 β in horizontal and amacrine cell development. More recently, our lab has created of double conditional AP-2 α /AP-2 β KO mutant model in the retina, due to the acquisition of the “floxed” AP-2 β mouse line.

These double conditional KO mice ($AP-2\alpha^{lacZki/lox}/AP-2\beta^{BKO/lox}$) only display defects in the developing retina and survive past birth and into adulthood allowing for complete examination of retinogenesis. Studies thus far performed on post-natal double conditional mutants confirmed a complete loss of horizontal cells in the INL in Cre-positive regions of the peripheral retina (Zaveri, M., unpublished data). After two months, mutants displayed a thinning of the outer plexiform layer (OPL), and it is suspected that this is a direct result of the loss of horizontal cells as the OPL would normally house photoreceptor terminals, horizontal cell and bipolar cell synapses (Zaveri, M., unpublished data).

The NCC population also serves as a major site of *Tcfap2* expression, especially in the eye. At E8.5 AP-2 mRNA is found to be present in neural folds and head mesenchyme, and subsequently after is found in neural crest populated tissues such as PNS ganglia and facial/brachial arch mesenchyme. Distribution of AP-2 mRNA in the facial mesenchyme is found to be consistent with expression in cranial neural crest-derived mesectoderm, that will give rise to facial connective tissues and skeletal elements (Mitchell, Timmons et al. 1991). *Tcfap2* expression continues to be strong in post-migratory NCC derived structures and germline $AP-2\alpha^{-/-}$ KO mice die perinatally, displaying failure of closure of the dorsomedial cranial folds, abnormalities in craniofacial morphology, failure in cranial ganglia development and neural tube closure defects leading to exencephaly (Schorle, Meier et al. 1996, Zhang, Hagopian-Donaldson et al. 1996).

$AP-2\alpha$ is seen as vital for neural crest specification in *Xenopus*, and it is hypothesized that deformities arising in NCC populations absent of $AP-2\alpha$ is a result of

failed specification of NCC progenitors rather than aberrations in differentiation or migration (Luo, Lee et al. 2003). Early expression of *Tcfap2α* is overlapped with *Tcfap2β* beginning at E8, diverging and creating distinct expression patterns around E11. Both AP-2α and AP-2β are also found to be expressed in the NCC derived mesenchymal cells that surround the lens placode (West-Mays, Zhang et al. 1999) however by E15.5 the expression of AP-2β is much greater in the POM in comparison to AP-2α (Figure 5).

There are two known human conditions that are related to mutations of the human *TFAP2* genes. A mutation in the human *TFAP2A* gene is linked to Branchio-Oculo-Facial Syndrome (BOFS), a genetic condition that is characterized by various craniofacial abnormalities including skull deformities, abnormal nasal tips and cleft lips (Milunsky, Maher et al. 2008). BOFS occurs when a missense mutation in the *TFAP2A* gene alters the amino acid sequence in the DNA binding domain, resulting in a non-functional transcription factor this is unable to properly homo- or heterodimerize with normal AP-2 proteins, reducing overall AP-2 function. BOFS patients who have a deleted *TFAP2A* allele exhibit milder symptoms than patients with missense mutations, suggesting a dominant negative effect due to the missense mutation (Milunsky, Maher et al. 2008, Milunsky, Maher et al. 2011). Eye deformities also occur including, anophthalmia, microphthalmia, coloboma of the iris, retina or ON, observed in both BOFS patients and AP-2α^{-/-} mice (Milunsky, Maher et al. 2008, Stoetzel, Riehm et al. 2009, Aliferis, Stoetzel et al. 2011).

The second human condition is Char syndrome, which occurs due to an autosomal dominant mutation affecting the AP-2β transcription factor and is characterized by a

patent ductus arteriosus, facial dysmorphism and abnormalities of the fifth digit (Satoda, Zhao et al. 2000). Identified mutations of the *TFAP2B* gene that result in Char syndrome include missense mutations within the highly conserved basic domain that impede binding of AP-2 target sequences and a missense mutation in the PY motif of the transactivation domain (Satoda, Zhao et al. 2000, Zhao, Weismann et al. 2001). Although the eye has not been examined in detail in patients with Char syndrome, structures that are affected, such as the patent ductus arteriosus, are derived from neural crest origin, speaking to the importance of AP-2 β expression in the development of structures contributed to by the neural crest.

Collectively, the data suggests requirement for AP-2 β expression in NCCs during the development of the anterior segment of the eye and warrants further study of its role and significance during embryonic development.

CHAPTER TWO

RATIONALE, MAIN HYPOTHESIS & RESEARCH AIMS

2.1 Rationale for the study

The development of structures within the anterior segment is vital for proper physiological function of the eye, and when these structures are malformed they can initiate the beginning of irreversible disease processes such as the loss of RGCs leading to glaucoma. A variety of ASDs exist in humans, and can be categorized as ASDs that arise from abnormalities of neural crest derived structures (ASD^{nc}), and ASDs arising from malformed structures not derived from NCCs (ASD^{non-nc}). Importantly, 50% of patients with ASD will also develop glaucoma as a result of the malformed tissues. Multiple genes govern the differentiation and migration patterns of the cranial NCCs, which contribute to the POM that gives rise to structures of the anterior segment, and require further study. Investigation of the role of the AP-2 transcription factor family in eye development has been the focus of our laboratory for a number of years. Interestingly, initial expression of the AP-2 transcription factors during embryogenesis can be found in premigratory NCCs and their derivatives. In particular, AP-2 β (*Tcfap2 β*) is highly expressed in the POM that gives rise to anterior eye tissues, and it is likely that absence of its expression would negatively impact development of these structures. Homozygous germline KO of *Tcfap2 β* in mice results in death shortly after birth, demonstrating its requirement in development. These mutants are therefore not conducive for studying the development of the anterior eye structures since substantial differentiation of these structures occurs after birth. In order to circumvent this our lab is able to utilize Cre loxP technology to restrict deletion of *Tcfap2 β* to the NCC population, allowing for the examination of these structures post-natally. Generating a novel mouse model with conditional deletion of AP-

2 β in NCCs will assist in elucidating AP-2 β 's role in the complex genetic cascade governing anterior eye development and enhance our knowledge of the basis of ASD and associated ocular diseases such as glaucoma.

2.2 Main Hypothesis

Conditional deletion of AP-2 β in cranial neural crest cell populations results in dysgenesis of the anterior segment of the eye, leading to glaucomatous changes.

2.3 Research Aims

2.3.1 Generate a mouse model in which AP-2 β is conditionally deleted in the cranial NCC population contributing to the development of the anterior segment of the eye and examine abnormalities found in embryonic and post-natal eyes of AP-2 β NCC KO mutants via histological, immunofluorescent and live imaging techniques.

Since development of the anterior segment of the eye continues post-natally and a global homozygous KO of AP-2 β results in death shortly after birth, a breeding scheme was designed that incorporates Cre loxP technology to create a conditional KO of AP-2 β in the NCC of the eye, enabling examination of the development of the anterior chamber past birth. Three mouse lines will be utilized to restrict deletion of AP-2 β to the NCC population, as summarized in Figure 6. Immunohistochemistry will be employed to confirm deletion of AP-2 β in the NCCs that contribute to the POM and structures of the anterior chamber in embryonic (E15.5 and E18.5) AP-2 β NCC KO mutants. Histological

examination of anterior eye structures of AP-2 β NCC KO mutants and their wildtype littermates at stages E10.5, E15.5, E18.5 and P42 will be performed in order to determine if absence of expression of AP-2 β in the neural crest has negatively impacted the structural formation of derivative tissues within the anterior chamber. Live imaging equipment will allow for the confirmation of the presence of any abnormalities found in histological samples, to further confirm that they did not arise due to processing and/or sectioning artifact.

2.3.2 Measure intraocular pressure of the AP-2 β NCC KO mutants and compare with wildtype littermates.

The anterior segment of the eye is responsible for regulating aqueous outflow and consequently IOP. Previous studies have shown that malformations in structures and/or the outflow pathway, as seen in many models of ASD, can result in glaucoma. Due to the suspected abnormalities of the anterior chamber structures of the AP-2 β NCC KO mutants, IOP will be measured using a rebound tonometer (TonoLab, Vantaa, Finland) to determine if it exceeds normal ranges, suggestive of a disruption of aqueous humour drainage.

2.3.3 Conduct retinal ganglion cell counts and axonal counts of ONs of the post-natal eyes of the AP-2 β NCC KO mutants and compare with wildtype littermates.

Immunofluorescence and electron microscopy will be used to examine the RGC population and their axons respectively to determine if alteration in outflow dynamics has reduced the number of RGCs in the retina and their axons within the ON. Additionally the cross-sectional area of the ONs will be measured to further prove loss of RGC axons. RGCs and associated ON axons will be quantified to determine if there has been a significant loss of these cells in the AP-2 β NCC KO mutants relative to their wildtype littermates.

CHAPTER THREE
EXPERIMENTAL DESIGN

3.1 Animal Husbandry

All experiments were performed at McMaster University and animals were housed at the Central Animal Facility in a Level D classified room. The environment of the room was regulated to 22°C with a 12-hour light:dark cycle. Mice were housed in cages with dry bedding, enrichment and ad libitum access to both food (Harlan 8640 5% fat) and water. All animal procedures were performed in accordance with the ARVO Statement for the Use of Animals in Ophthalmic and Vision Research. For genotyping, DNA was extracted from adult ear clippings using the EZNA Tissue DNA Kit (Omega Bio-Tek). Genotypes were determined by previously established polymerase chain reaction (PCR) protocols (Table 1).

3.2 Generation of AP-2 β NCC KO mutants

The series of crosses used to generate AP-2 β NCC KO mutants are depicted in Figure 6. Two *Tcfap2 β* alleles were incorporated into the breeding scheme including a *Tcfap2 β* ^{BKO/+} null allele (due to a germline insertion of a phosphoglycerokinase (PGK)-neo cassette disrupting exon 4) (Moser, Pscherer et al. 1997) and a *Tcfap2 β* ^{lox} allele (where exon 6 of *Tcfap2 β* is flanked by single loxP sites). The initial cross of the mating scheme began with female mice heterozygous for AP-2 β ^{BKO/+} paired with heterozygous male Wnt1-Cre^{+/-} transgenic mice (Danielian, Muccino et al. 1998). Wnt-1/GAL4/cre-11 transgenic mice were purchased from Jackson Laboratory (Stock number 003829) and bred with C57Bl/6. The promoter/regulatory sequences of the Wnt-1 gene were used to restrict the expression Cre-recombinase to the embryonic neural tube, and subsequently

the NCC population beginning at E8.5. Only male breeders carrying the Cre transgene were used in order to minimize any variability of Cre excision patterns due to parent-of-origin (as has been seen in other Cre lines (Heffner, Herbert Pratt et al. 2012)). The male offspring that genotyped AP-2 β ^{BKO-/+} / Wnt1-Cre^{+/-} were then bred with female homozygous AP-2 β ^{lox/lox} mice to produce a progeny in which one quarter would theoretically be AP-2 β ^{BKO-/lox} / Wnt1-Cre^{+/-} and have AP-2 β deleted specifically from the NCC population. Littermates used as controls were gender matched and either contained two functional copies of *Tcfap2 β* in the NCC population or were missing one functional copy of *Tcfap2 β* if the former was not available.

3.3 Histology

The dissected whole eyes of the AP-2 β NCC KO mutants were either shipped from our collaborator or collected in our laboratory. Tissue was fixed in 10% neutral buffered formalin for 24 hours then stored in 70% ethanol. Samples were processed (Histology Department, McMaster University) and embedded in paraffin (Paraplast Tissue Embedding Media, Fisher Scientific, Waltham, MA). Serial sections were cut to 4 μ m in thickness and used for immunofluorescent analysis or hematoxylin and eosin (H&E) staining.

3.4 Immunofluorescence

Indirect immunofluorescence was performed using the following primary antibodies: Mouse anti-AP-2 α 1:1 (DHSB), rabbit anti-AP-2 β 1:50 (Cell Signaling),

mouse anti-N-cadherin 1:100 (BD Transduction), mouse anti- α -smooth muscle actin 1:100 (Sigma F3777), rat anti-endomucin 1:100 (eBioscience), goat anti-Brn3a 1:100 (Santa Cruz), and mouse anti-GFAP 1:1000 (Sigma-Aldrich). Fluorescent secondary antibodies used were Alexa Fluor 488 or 568 (Invitrogen – Molecular Probes, Burlington, ON) at 1:200 for one hour at room temperature.

Paraffin-embedded sections were deparaffinized in xylene, hydrated (through 100%, 95% and 70% ethanol, followed by water), treated with 10mM sodium citrate buffer (pH 6.0; boiling for 20 minutes) for antigen retrieval, blocked with normal serum (one hour) and incubated with primary antibodies overnight at 4°C. For all co-localizations, primary and secondary antibodies were mixed and incubated simultaneously. All stains were mounted with ProLong Gold antifade reagent containing 4,6-diamino-2-phenylindole (DAPI) (Invitrogen – Molecular Probes, Burlington, ON). All staining was visualized with a microscope (Leica, Deerfield, IL) equipped with an immunofluorescence attachment, and images were captured with a high-resolution camera and associated software (Open-Lab; Improvision, Lexington, MA). Images were reproduced with image-management software (Photoshop 7.0; Adobe Systems Inc., Mountain View, CA).

3.5 Anterior Segment Imaging with the Phoenix Micron IV Imaging Microscope and OCT attachment

AP-2 β NCC KO mutants and their wildtype littermates were weighed and anesthetized with an intraperitoneal (i.p.) injection of 2.5% avertin at 0.015 ml/g body weight. Whiskers were trimmed to ensure no obstruction of the imaging system and two

sets of eye drops applied in order to dilate the pupils (0.5% Tropicamide Ophthalmic Solution and 2.5% Phenylephrine Hydrochloride Ophthalmic Solution, AKORN, Lake Forest, IL, USA). The corneas were maintained well moistened throughout the procedure with consistent application of Tear-Gel ophthalmic liquid gel (Alcon Canada, Mississauga, ON, Canada) in order to prevent drying. The Phoenix Micron IV rodent eye imaging system, with optical coherence tomography (OCT) attachment (Phoenix Research Labs, Pleasanton, CA, USA) was utilized in order to image the corneas and anterior chambers of the AP-2 β NCC KO mutants and their wildtype littermates.

3.6 IOP measurements

Three-month-old AP-2 β NCC KO mutants and their wildtype littermates were weighed and anesthetized with an i.p. injection of 2.5% avertin at 0.015 ml/g body weight. LACRI-LUBE (Allergan Inc., Markham, ON, Canada) was applied to the eyes to maintain a moist tear film and whiskers were trimmed so there was no impediment of the probe. A validated commercial rebound tonometer (TonoLab, Vantaa, Finland) was mounted on a retort stand with the probe aligned horizontally and perpendicularly to the central cornea, with the tip positioned between 2-3mm from the eye as previously advised (Chatterjee, Oh et al. 2013). Ten means of six measurements were collected per eye that would be used to calculate an overall mean. Measurements were only accepted if they registered as TonoLab readings with the best reproducibility (no bar symbol) or the next best reproducibility (bar present at the bottom of the screen) as per the manufacture manual. All measurements were taken between 13:00 to 15:00 in the afternoon and three

minutes after injection of avertin, as this has been previously shown to be a period of stable IOP (Ding, Wang et al. 2011).

3.7 RGC tracing with Neurobiotin

The animal was deeply anesthetized and the eyes enucleated. ONs were collected (See 3.8 Electron Microscopy) and eyeballs were placed cornea down in a moist, warm, oxygenated chamber. A piece of gelfoam soaked in 8% Neurobiotin (NB) (Vector Laboratories, Inc. Burlington, CA 94010) was placed on the optic stump. The eyeballs were incubated in the chamber for one hour, after which they were fixed for two hours in 4% paraformaldehyde. After washes, the retinae were removed and incubated in Texas Red Conjugated Streptavidin (Jackson ImmunoResearch Laboratories, Inc.) overnight at room temperature. The next morning the retinae were washed and mounted onto slides with Vectashield containing DAPI (Vector Laboratories, Inc. Burlington, CA 94010). All staining was visualized with a microscope equipped with an immunofluorescence attachment (Zeiss, Germany), and images were captured with a high-resolution camera and associated software (Zen; Zeiss, Germany). Images were reproduced with image-management software (Photoshop 7.0; Adobe Systems Inc., Mountain View, CA).

3.8 Electron Microscopy

ONs were carefully dissected from the ocular orbit and immediately immersed in a solution of 4% PFA/2% Glutaraldehyde for two hours. Sample were then washed in phosphate buffer solution and post fixed in a 1:1 solution of 2% aqueous OsO₄/0.1M Cacodylate Buffer for one hour at room temperature. Serial dehydration occurred in

acetone (20%, 50%, 75%, 90% and 100%), and samples were embedded in EPON resin. Thin sections were created using a diamond knife with an ultramicrotome (Reichert-Jung Ultracut E Microtome; American Instruments) and collected on 200 mesh copper grids (Electron Microscopy Sciences, McMaster University). Sections were stained with uranyl acetate and Reynolds' lead citrate and viewed using a JEOL 1200EX electron microscope at an accelerating voltage of 80kV. Images were collected and stored for later analysis and quantification.

3.9 Quantification and Statistical Analysis

Retinal thickness measurements were taken from P42 H&E stained slides using ImageJ (NIH) for quantification. Retinal wholemounts with DAPI labeled nuclei and NB labeled RGCs were sampled four times in the mid-periphery of each petal, the counts of the nuclei were tallied and averaged to be considered as one sample. Five samplings of each ON were obtained, axon numbers tallied and averaged to be considered one sample. Quantification of the nuclei, RGCs and axons was performed using the manual "Cell counter" plug-in with quantification software ImageJ (NIH) in order to ensure each soma/axon was counted only once and an automatic tally was generated. Comparisons of IOP measurements, retinal thickness, DAPI and RGC counts on retinal wholemounts and ON samplings between AP-2 β NCC KO mutants and wildtype littermates were tested for significance with a Student's two-tailed *t*-test (Prism 6, GraphPad Software, La Jolla, CA, USA). Data was considered significant when $p < 0.05$. All values are expressed as mean \pm SD (standard deviation).

Table 1. PCR protocols

Alleles	Primers	PCR conditions	Products
Wnt1Cre	Cre1 5'-GCT GGT TAG CAC CGC AGG TGT AGA G-3' Cre3 5'-CGC CAT CTT CCA GCA GGC GCA CC-3'	45s at 95°C, 1min at 67°C, 1min 10s at 72°C for 33 cycles	Presence of Cre transgene 420bp
βGal	9684 Fwd 5'-TAA GAG GCC TAT AAG AGG CGG-3' 9685 Rev 5'-ATC AGT CTC CAC TGC AGC-3'	45s at 95°C, 1min at 67°C, 1min 10s at 72°C for 33 cycles	Presence of GAL4 transgene 600bp
AP-2β ^{KO/+} vs AP-2β ^{+/+}	PGK-PolyA DW 5'-CTG CTC TTT ACT GAA GGC TCT TT-3' 4 Exon Rev 5'-TTC TGA GGA CGC CGC CCA GG-3' 4 Exon DW 5'-CCT CCC AAA TCT GTG ACT TCT-3'	45s at 95°C, 45s at 58°C, 1min at 72°C for 37 cycles	<i>Tcfap2β</i> - 380bp <i>Tcfap2β</i> + 221bp
AP-2β ^{lox} vs AP-2β ^{+/+}	BFL1 5'-GTC TGT TTA GAA CCT GGC TCA GCC AG-3' BFL2 5'-TCT GGC AAG GCT CTT TCG GGG CAC TC-3' SD5P33 5'-CGC AGC GCA TCG CCT TCT ATC GCC TT-3'	2min at 95°C, 45s at 95°C, 3min at 70°C for 34 cycles	<i>Tcfap2β</i> lox 550bp <i>Tcfap2β</i> + 450bp

CHAPTER FOUR

RESULTS

4.1 Generation of AP-2 β NCC KO mutants

Since mice with a homozygous global deletion of *Tcfap2 β* die shortly after birth, conditional deletion of *Tcfap2 β* from the NCC population was achieved through use of the breeding scheme shown in Figure 6. Three mouse lines were utilized including AP-2 β ^{BKO-/+} heterozygotes with a global deletion of one allele as a result of a PGK-neo cassette disrupting exon 4 (Moser, Pscherer et al. 1997), AP-2 β ^{lox/lox} homozygotes with loxP sites flanking exon 6 and Wnt-1Cre transgenic mice that restrict expression of Cre recombinase to the embryonic neural tube and consequently NCCs (Danielian, Muccino et al. 1998). AP-2 β ^{BKO-/+} heterozygotes are incorporated into the breeding in lieu of only using the AP-2 β ^{lox/lox} homozygotes in order to ensure there is no dilution of the efficacy of the Cre-recombinase. All progeny from the final cross were genotyped for the alleles *Tcfap2 β* ⁺, *Tcfap2 β* ^{lox} and presence of the Cre using PCR (Figure 7). To ensure deletion of *Tcfap2 β* in the NCC population of the mutants, immunohistochemistry was performed to detect expression of AP-2 β in the POM of E15.5 and E18.5 mutant embryonic eyes. Although the Cre is expressed earlier on, stage E15.5 was chosen as the expression patterns of *Tcfap2 α* and *Tcfap2 β* have now begun to diverge at this stage, with expression of AP-2 β found to be strong in the NCCs contributing to the POM and corneal stroma (Figure 5). At E15.5 the wildtype eye stained positively for AP-2 β expression in the POM, the developing retina, the corneal stroma, corneal epithelium and eyelid epidermis (Figure 8A). The wildtype E18.5 embryo also exhibited positive AP-2 β staining in the POM, the corneal epithelium, endothelium and stroma and the developing retina (Figure 8C). In comparison, expression of AP-2 β in the mutants was absent in the POM, and

corneal endothelium and stroma, whereas expression was retained in the developing retina and corneal epithelium (Figure 8B,D). This demonstrates that AP-2 β was deleted only in NCC-derived tissues. Mendelian genetics suggests a ratio of $\frac{1}{4}$ mutants per litter however in practice it was found to be much lower, thereby necessitating a large number of breeder cages. In addition, often times the mutants tended to be runty and developed malocclusions resulting in premature death. This is likely due to the conditional deletion of AP-2 β in additional NCC populations that are contributing to other organ systems (such as the cardiac NCC contributing to the developing cardiac outflow tract and ductus arteriosus) within the embryo. To minimize the loss of mutants, a system was devised in conjunction with the room technicians in the Central Animal Facility to closely monitor their conditions and provide recovery gel and treatment when needed.

4.2 Histological examinations of AP-2 β NCC KO embryonic and adult mutants

Although the Wnt1-Cre is first expressed at E8.5, we examined embryonic stages beginning at E10.5 as this marks the first presence of NCC migration into the presumptive anterior chamber (Gage, Rhoades et al. 2005). Paraffin sections of E10.5 and E15.5 were stained with H&E to determine if any histological abnormalities of the POM resulted due to the deletion of *Tcfap2 β* . Embryonic stages of E10.5, just after the lens vesicle has pinched off from the overlying surface ectoderm and the POM is migrating into the presumptive anterior segment, of mutants and wildtype littermates looked remarkably similar, with no suggestion of abnormal development due to the conditional deletion (n=4) (Figure 9A-B). Conversely at E15.5, once the cornea has formed from the

POM and the second wave of mesenchyme has reached the iridocorneal angle, the mutant cornea appeared to be more diffuse with large gaps within the stroma and the cornea and lens appearing to be attached (n=2) (Figure 9C-D, arrowheads).

Upon initial examination of adult (P42) AP-2 β NCC KO mutant eyes (n=8) multiple malformations within the anterior chamber were apparent. The most striking was the disruption of the iridocorneal angle with the iris adherent to the cornea, creating a highly penetrant (n=8) closed angle phenotype (Figure 10A-B). The adherence between the iris and cornea was confirmed to be consistent 360° throughout the eye with OCT imaging of the anterior eye chambers of anaesthetized mice (n=6) (Figure 11). The ciliary body was also malformed, as it appeared rudimentary in the mutants lacking its normally convoluted and lobulated structure (n=6) (Figure 10A-B). Upon closer examination of the cornea, the corneal endothelium, which is a derivative of the POM, appeared to be absent (Figure 10C-D). To confirm this an endothelial marker N-cadherin (n=8), a calcium dependent glycoprotein highly expressed by the corneal endothelium, was used (Reneker, Silversides et al. 2000). Immunostaining for N-cadherin revealed that there was no apparent expression in the posterior corneal region of the mutants, whereas wildtype littermates had a clearly defined corneal endothelium staining positive for N-cadherin (Figure 12A-B). To determine whether the absence of the corneal endothelium in the adult mutants occurred as a developmental defect, mutant E18.5 sections were also examined with both H&E and immunofluorescence and similarly showed a lack of endothelial cells and absent N-cadherin staining (n=6) (Figure 13).

The corneal stroma, which is also populated by the NCC, appeared hypercellular in the AP-2 β NCC KO mutants and also lacked the normal arrangement of collagen fibrils observed in wildtype littermates (n=8) (Figure 10C-D). This phenotype likely accounted for the corneal clouding observed in the mutants. In addition, upon gross examination of the mutant eyes *in vivo*, red vessels were apparent suggesting evidence of corneal neovascularization (Figure 14). Further imaging of the anterior chamber with OCT confirmed the presence of vessel foramen in the corneal stroma (Figure 11, red arrowheads). In addition, sections of AP-2 β NCC KO mutant corneas displayed positive staining for endomucin, a sialomucin specifically expressed by the endothelium of blood vessels (Figure 14A-B, arrows). Importantly, this staining was not observed in wildtype littermates. Lastly, embryonic histological sections at E18.5 also revealed the presence of red blood cells in the corneal stroma of the AP-2 β NCC KO mutants and not in wildtype littermates, suggesting that conditional deletion of AP-2 β resulted in loss of the angiogenic privilege normally observed in the cornea (Figure 13B, D, arrowheads).

Interestingly the corneal epithelium, a derivative of the surface ectoderm, was reduced from a 4-5 cell stratified squamous epithelial layer to two cell layers (n=8) in the AP-2 β NCC KO mutants (Figure 10C-D). In addition, some of the mutant lenses (n=4) exhibited evidence of anterior subcapsular cataracts (ASC) that stained positive for α -smooth muscle actin, a marker of myofibroblasts, indicative of the development of ASC (Figure 12C-D). Since neither of these tissues are derived from the NCC population it is suspected that they have arisen as a secondary defect (see Discussion).

4.3 Increased IOP in AP-2 β NCC KO mutants relative to wildtype littermates

Obstructions of the aqueous outflow pathway is known to lead to elevations in IOP in a variety of inducible and spontaneous mouse models of glaucoma (as reviewed in (McKinnon, Schlamp et al. 2009)). In order to determine if the closed angle phenotype of the AP-2 β NCC KO mutants resulted in elevated IOP, rebound tonometry was used on a cohort of AP-2 β NCC KO mutants and their wildtype littermates. A significant elevation of IOP was readily apparent in three-month-old AP-2 β NCC KO mutants. The wildtype littermate control mice had an IOP measuring 9.76 ± 1.88 mmHg (n=12 eyes), a value consistent with previous measures of noninvasive IOP readings in 3-month-old C57Bl/6 background strains (Kipfer-Kauer, McKinnon et al. 2010). In contrast, AP-2 β NCC KO mutants had a significant elevation of IOP measuring 28.87 ± 5.19 mmHg (n=12 eyes, $P < 0.0001$, Student's two-tailed t -test) (Figure 15), a value that is similar to IOP measurements reported in a previously published genetic animal model of glaucoma (Mao, Hedberg-Buenz et al. 2011). This data supports that the closed angle phenotype observed in the AP-2 β NCC KO mutants resulted in disruption of the aqueous outflow pathway that leads to an increase in IOP. Such an environment is favourable to the development of glaucomatous retinal damage.

4.4 Decreased retinal thickness in P42 AP-2 β NCC KO mutants

Upon examining H&E stained sections of the AP-2 β NCC KO mutant retinae at P42 the overall thickness appeared to be decreased. Total measurement of all retinal layers revealed that the mutant retinae were indeed significantly thinner ($218.56\mu\text{m} \pm$

7.90, n=4 retinae) relative to that of their age-matched littermates ($243.47\mu\text{m} \pm 7.38$, n=4 retinae, $P < 0.005$, Student's two-tailed *t*-test) (Figure 16). Although initially this would appear to suggest total retinal degeneration, which is not a typical consequence of glaucoma, further measurement of the outer nuclear layer (ONL), inner nuclear layer (INL), and inner plexiform layer (IPL) revealed that the overall retinal thinning was mainly due to thinning of the IPL, the layer that contains the dendrites of RGCs. The IPL of the mutants ($56.11\mu\text{m} \pm 5.00$, n=4 retinae) was significantly thinner than wildtype littermates ($74.67\mu\text{m} \pm 4.80$, n=4 retinae, $P < 0.005$, Student's two-tailed *t*-test)(Figure 16). In comparison, the ONL and INL, the layers that contain the nuclei of the photoreceptors and the nuclei of amacrine, bipolar and horizontal cells respectively, exhibited no significant difference in thickness in the mutant and wildtype littermates. This finding suggests that the thinning of the mutant retinae at six weeks of age may have been the result of a loss of RGCs as the layer that contains their dendrites is significantly reduced.

4.5 Loss of RGCs in two-month old AP-2 β NCC KO mutant retinae relative to wildtype littermates

To determine if the increase in IOP in AP-2 β NCC KO mutants resulted in a loss of RGCs, the retinal cell type affected in glaucoma, two methods for assessing RGC number were employed. Initially, a primary antibody targeting transcription factor Brn3a, a marker specific to RGCs in mice, was used on radial sections of the retina. During murine retinal development the POU-domain Brn3 transcription factor family members have been shown to play vital roles in cell differentiation, survival and axonal elongation

(Wang, Mu et al. 2002). Family member Brn3a has been shown to be a reliable marker for identifying both naïve and optic nerve-injured RGCs (Nadal-Nicolas, Jimenez-Lopez et al. 2009). In order to confirm that the conditional deletion of AP-2 β in NCCs did not affect the initial development of RGCs, embryonic (E18.5) AP-2 β NCC KO mutant sections were stained with Brn3a and displayed positive staining for RGCs in the inner neuroblast layer of the developing retina (data not shown). Adult retinas were then examined post-natally (P42) and the AP-2 β NCC KO mutants showed no staining of RGCs soma in the GCL (n=7)(Figure 17), unlike their wildtype littermates that did, suggesting a loss/degeneration of RGCs by this P42 time point. Since Brn3a is a transcription factor, it is indeed possible that its expression may have been downregulated in the AP-2 β NCC KO mutants and RGCs are still present. Thus, to further confirm our findings, an alternate RGC labeling method was utilized (Pang and Wu 2011). Neuronal tracer Neurobiotin (NB) was placed upon the ON stump to be taken up and transported retrogradely by the RGC axons to the cell bodies. Fluorescence microscopy of NB labeled RGCs in retinal wholemounts displayed stark contrast between AP-2 β NCC KO mutants and wildtype littermates with significantly fewer RGCs and their axons in the mutant group (Figure 18). It was interesting to note the segmental reduction of RGC axons in a fan-shaped pattern on the retinal wholemounts, a phenotype that is similar to what has been observed in the most well characterized mouse model of glaucoma, the DBA/2J inbred line (Jakobs, Libby et al. 2005). Manual counting of DAPI labeled nuclei and NB labeled RGC somas was performed using ImageJ software and revealed that wildtype littermates had on average 10163 ± 1603 nuclei/mm² and 4244 ± 365 RGC/mm² (n=4

retinae), values consistent with total neuronal counts in the GCL and the calculation that 43% of cells in this layer are RGCs (Jeon, Strettoi et al. 1998). Cell counts of AP-2 β NCC KO mutant retinae showed significantly fewer cells with 6505 ± 511 nuclei/mm² and 2769 ± 462 RGC/mm² (n=4 retinae, P = 0.0048 and P = 0.0024 respectively, Student's two-tailed *t*-test) (Figure 19). These data demonstrate that by two months of age the AP-2 β NCC KO mutants have exhibited a substantial loss of RGCs, which was likely due to the increased IOP (previously demonstrated in section 4.3).

Within the GCL of the retina two major cell types exist including the RGCs and displaced amacrine cells (dACs), interneurons that play an important role in inner retinal visual processing and account for 57% of the cells in the GCL (Jeon, Strettoi et al. 1998). Therefore from the previous quantifications of cells in the GCL (above) the number of dACs is calculable by subtracting the number of RGCs by the total number of nuclei present in the GCL. The number of dACs in wildtype littermates was determined to be 5774 ± 1178 dACs/mm² with the AP-2 β NCC KO mutant retinae having a significantly lower number of dACs at 3641 ± 755 dACs/mm² (n=4 retinae, P = 0.0225, Student's two-tailed *t*-test). These data suggest that there is also loss of amacrine cells at two-months of age (Figure 19).

4.6 Loss of retinal ganglion cell axons in ONs

To further reveal evidence of glaucomatous damage in the AP-2 β NCC KO mutants, cross-sections of ONs (which contain the axons of the RGC bodies found in the GCL) from the corresponding two-month old retinae seen in section 4.5 were analyzed

with electron microscopy. The ONs of the wildtype littermates appeared healthy with many axons of various sizes closely compacted and surrounded by myelin sheaths (Figure 20A). The ONs of the AP-2 β NCC KO mutants however had a decreased number of myelinated axons, presence of degenerating axons (Figure 20A, arrow) and areas of severe atrophy (Figure 20A, asterisk). Quantification of the total number of axons also revealed a significant reduction in the number of ON axons in the AP-2 β NCC KO mutants with 6365 ± 4284 total number of axons/ON (n=4 ONs) when compared to wildtype littermates that averaged 36143 ± 7276 total number of axons/ON (n=4 ONs, P = 0.0004, Student's two-tailed *t*-test) (Figure 20B). As a consequence of the loss of axons, the cross-sectional area of the mutant ONs was significantly reduced ($31,871 \pm 10,275 \mu\text{m}^2$, n=4 ONs) 51% less relative to their wildtype littermates ($62,286 \pm 11016 \mu\text{m}^2$, n=4 ONs, P = 0.0068, Student's two-tailed *t*-test), further supporting that the AP-2 β NCC KO mutant ONs have undergone severe glaucomatous progression (Figure 21).

4.7 Increased glial reactivity of the retina

Following CNS injury and disease, such as what occurs in glaucoma, hypertrophy and proliferation of glial cells such as Müller glia and astrocytes will occur, also known as gliosis. A hallmark of gliosis is the upregulation of intermediate filaments, such as glial fibrillary acidic protein (GFAP), that are in contact with the cytoskeleton and extracellular matrix and will facilitate the rapid and long-term remodeling of tissue structure. In the wildtype littermates normal GFAP staining of astrocytes is seen in the nerve fiber layer (NFL) and GCL, with no staining of Müller glia in the other retinal

layers as expected (Figure 22A)(Bjorklund, Bignami et al. 1985, Sarthy, Fu et al. 1991). AP-2 β NCC KO mutants however exhibited an upregulation in expression of GFAP in the Müller glia, similar to what has been previously observed in animal models of glaucoma (Tanihara, Hangai et al. 1997, Wang, Tay et al. 2000) (Figure 22B).

CHAPTER FIVE

DISCUSSION, FUTURE DIRECTIONS & CONCLUSION

DISCUSSION

In humans, mutations in the *TFAP2B* gene leads to a series of congenital abnormalities collectively referred to as Char syndrome. These patients present with congenital defects of structures contributed to by NCCs such as the cardiac outflow tract and facial mesenchyme resulting in a patent ductus arteriosus and distinctive facial deformities respectively (Satoda, Pierpont et al. 1999, Satoda, Zhao et al. 2000). To date, there are no reports of incidences of glaucoma in Char syndrome patients; however this is likely due to the fact that detailed ocular examinations of patients have not been carried out. It has been well established that the NCC population, alongside mesoderm, contributes to the POM that is responsible for the proper development of structures found in the anterior segment of the eye (Johnston, Noden et al. 1979, Gage, Rhoades et al. 2005). Numerous genes, including *FOXC1* and *PITX2*, are expressed in the POM during development and subsequently structures found in the anterior segment. A variety of mouse models with mutations in genes expressed in the POM exhibit improper development of structures of the anterior eye and have been linked to congenital syndromes in humans that have developmental defects of the anterior segment often leading to glaucoma, such as Axenfeld-Rieger anomalies (Kidson, Kume et al. 1999, Smith, Zabaleta et al. 2000, Lines, Kozlowski et al. 2002, Evans and Gage 2005). *Tcfap2 β* is highly expressed in the NCC population and findings for the AP-2 β NCC KO mutants demonstrate the importance of its expression during the development of structures in the anterior eye segment. Of the malformations observed in our mouse model the highly penetrant closed iridocorneal angle phenotype proved most interesting

as it presumably disrupted the aqueous outflow pathway within the eye, causing an increase in IOP and subsequent loss of RGCs and their axons. Together these data identify the AP-2 β NCC KO mutant as a potential new mouse model of glaucoma.

5.1 AP-2 β expression in NCCs and the development of the anterior eye segment

The development of the anterior chamber of the eye has been extensively studied with tissue derivations of each structure well defined. It is now well established that the NCC population, alongside mesoderm, will compose the POM that will ultimately contribute to the corneal stroma, corneal endothelium, iris stroma, ciliary body muscle, ciliary body stroma and trabecular meshwork of the anterior eye (Gage, Rhoades et al. 2005). However, little is known about the molecular and genetics events that regulate the development of these structures. A variety of genes are expressed in the NCC population and have been shown to be vital to the development of structures to which they contribute. *Tcfap2 β* is a gene that is neural crest-related but due to the lethality of the global AP-2 β ^{-/-} mutation in mice, its significance during the development of the anterior chamber was previously unknown, as these structures continue to develop up to three weeks after birth. By restricting the deletion of AP-2 β to the NCC population, allowing for viability of the mutants, we were able to examine, for the first time, the significance of its expression in the development of anterior eye structures.

Multiple malformations of the anterior segment presented in the AP-2 β NCC KO mutants, of which the most striking was the highly penetrant adhesion between the cornea and iris. This closed angle phenotype was consistently observed, with full adhesion of the

iris to the cornea in all mutants examined. It is unknown if this defect is a result of failure of separation between the iris and cornea during development or due to the additional malformations found in other anterior structures. For example, the AP-2 β NCC KO mutants also exhibited a variety of corneal phenotypes, including, a missing corneal endothelium, disorganization and neovascularization of the corneal stroma and reduced stratification of the corneal epithelium. The absence of an endothelium is likely a direct cause of the deletion of AP-2 β in the NCC population since it is derived from the NCCs and was not found to be present during embryogenesis. Interestingly, the lack of a corneal endothelium may have further contributed to the highly penetrant closed angle phenotype and corneal abnormalities. As hypothesized by Reneker et al. (2000) interference with the development of the corneal endothelium initiates a sequence of developmental anomalies that can cause anterior segment dysgenesis (ASD). While the corneal endothelium mainly functions to regulate hydration and nutrition of the corneal stroma it is also thought to provide a barrier between the anterior chamber and the “sticky” extracellular matrix of the stroma (Waring, Bourne et al. 1982, Reneker, Silversides et al. 2000). Therefore, in the absence of this protective barrier the iris may have adhered to the exposed extracellular matrix resulting in the closed angle phenotype observed. In addition, evidence would suggest that the lack of corneal endothelium could have also influenced the malformations seen in the corneal stroma and epithelium of our mutants. Corneal edema and clouding (also evident in our mice) have been previously linked to a loss of N-cadherin (the major classic cadherin expressed in the adult mouse corneal endothelium) from the endothelium alongside the observation of disorganized collagen fibrils

(Vassilev, Mandai et al. 2012). This is hypothesized to be due to the loss of proper regulation of water and macromolecules from exiting and entering the corneal stroma. Reduced stratification of the corneal epithelium similar to the phenotype of the AP-2 β NCC KO mutants (presenting as a two-cell layer epithelium) has also been observed in other mouse models lacking a corneal endothelium (Reneker, Silversides et al. 2000, Vassilev, Mandai et al. 2012). Most interestingly, the corneal epithelium is seen to return to a 5-6-cell layer epithelium in areas of the cornea where the endothelium remained present (Reneker, Silversides et al. 2000). Together, this data suggests that the malformation of the corneal endothelium directly results due to the conditional deletion of AP-2 β from the NCCs and is likely a major determinant of some of the ASD observed. It also points to the importance of *Tcfap2 β* gene expression in NCCs during the development of the corneal endothelium. Whether the closed angle phenotype is a consequence of the absent endothelium or failure of proper separation of the cornea and iris during development remains to be determined. The use of a more specific Cre or a tamoxifen inducible-Cre (allowing for the regulation of onset of Cre recombinase expression) to conditionally delete *Tcfap2 β* specifically from the corneal endothelium would further clarify its role in the ASD observed.

The transparency on the cornea is critical for optimal optical performance, and its maintenance of avascularity, recently termed angiogenic privilege, is a necessity for proper visual function (Azar 2006). The AP-2 β NCC KO mutants exhibited loss of corneal transparency, along with corneal neovascularization and positive staining of an endothelial blood vessel marker within the corneal stroma. These data suggest that AP-2 β

expression in the NCC population is required in order to establish angiogenic privilege during the development of the cornea. The *Foxc1* and *Pitx2* genes, whose expression is already well established in the NCCs of the POM and implicated in the proper development of the anterior eye segment, have also been identified as critical in establishing and maintaining corneal avascularity. Mouse mutants that are homozygous null for *Foxc1* and *Pitx2* in NCCs also develop neovascularization of the cornea (Seo, Singh et al. 2012, Gage, Kuang et al. 2014). In addition, these mouse models exhibit similar anterior segment phenotypes as our AP-2 β NCC KO mutants including lack of formation of the corneal endothelium, disorganization of the corneal stroma and abnormalities of the corneal epithelium (Gage, Suh et al. 1999, Kidson, Kume et al. 1999). Furthermore, there is data that indicates a downregulation of the *Tcfap2 β* gene in the developing corneas of temporal *Pitx2*^{-/-} KO mice (Gage, 2015, personal communications). Given this evidence it is tempting to suggest that *Tcfap2 β* works alongside or is directly acted upon by *Pitx2* in the developmental network that regulates anterior segment formation. Together, these data demonstrate for the first time the consequences of homozygous deletion of AP-2 β from the NCC population during the development of the anterior eye segment. The AP-2 β NCC KO mutant is a novel mouse model of ASD highlighting the importance of expression of AP-2 β in the NCC of the POM during eye development.

5.2 AP-2 β NCC KO mutants as a model of glaucoma

Glaucoma is a multifactorial disease process whose molecular processes remain to be fully elucidated. The progression of glaucoma generally involves blockage of aqueous outflow leading to an increase in IOP of the anterior chamber. This increase in IOP translates to the posterior aspect of the eye where pressure is placed upon the retina and ON, particularly at the ONH, causing damage to the RGCs and their axons. Mouse models of glaucoma prove to be extremely useful in not only helping to determine the molecular and genetic interactions that occur during the disease process but also providing an avenue for testing future therapeutic treatments to arrest and potentially reverse retinal damage. As previously established, a variety of mouse models of glaucoma exist that can be grouped into inducible and spontaneous/genetic models. Of the few spontaneous/genetic mouse models that are used, such as the well-established DBA/2J inbred strain, our model provides a few distinct advantages. The first is the timeline at which our mutants begin to lose RGCs. Our data demonstrates loss of RGCs as early as six weeks of age with a significant loss calculated at two months of age, which we have proven multiple ways including Brn3a staining, retinal thinning of the IPL, NB RGC tracing, ON counts/cross-sectional area measurements and evidence of glial reactivity. This rapid loss is likely attributed to the profound increase in IOP that results from the severe iridocorneal adhesion that is presumably disrupting aqueous outflow. In contrast, spontaneous models such as the widely used DBA/2J inbred strain, myocilin and $\alpha 1$ subunit of collagen type I transgenic models do not begin to experience loss of RGCs until 6-12 months of age with only a modest elevation in IOP (Aihara, Lindsey et al.

2003, Libby, Anderson et al. 2005, Senatorov, Malyukova et al. 2006). Our model more closely mimics the considerable increase of IOP and early loss of RGCs of the genetic *Sh3pxd2b (nee)* mouse model (Mao, Hedberg-Buenz et al. 2011). This likely has to do with how the elevation of IOP occurs in each of these models. The mutations in the initial three models affect drainage structures within the iridocorneal angle. However the *nee* mice and our model present with an adhesion between iris and cornea during development that creates a closed angle phenotype, which is likely more severe in disrupting aqueous humour from reaching the drainage structures in the first place. This would in turn cause a quicker and more extreme elevation of IOP within these mice at a young age. It should be noted that an alternate outflow pathway exists within the eye termed the uveoscleral pathway, located posteriorly to the classic drainage structures of the eye (i.e. trabecular meshwork and Schlemm's canal) (Figure 1B) (Lindsey and Weinreb 2002). Aqueous humour will enter the extracellular spaces of the iris root traveling to the ciliary muscle, the anterior choroid and the adjacent sclera to ultimately pass into the extraorbital fat tissue and the lymphatic drainage system. Therefore due to the phenotypes of the DBA/2J inbred strain, myocilin and $\alpha 1$ subunit of collagen type I transgenic models, aqueous humour would still have access to the uveoscleral pathway to exit the eye, providing alternate regulation of IOP. A closed angle phenotype, as seen in our model and *nee* mice, would block access to both the trabecular meshwork/Schlemm's canal and the uveoscleral pathway, likely augmenting the substantial and severe increase in IOP. Overall, given the decreased timeline of disease progression this model is

attractive for researchers as it decreases experimental timeframes and the cost of housing animals.

The second advantage of our model lies in the highly penetrant phenotype observed in the AP-2 β NCC KO mutants and the aggressive nature of the glaucoma. The current “gold standard” glaucoma model, the DBA/2J inbred strain, have highly variable phenotypes with varying loss of RGCs therefore necessitating a large cohort of animals to be examined in order to gain significant data (Libby, Anderson et al. 2005).

Comparatively, all AP-2 β NCC KO mutants examined had a consistent and complete adhesion between the iris and cornea, that induces a substantial increase in IOP at an early age accompanied with a rapid and abundant loss of RGCs. It should also reiterated that the fan-shaped sectorial loss of RGCs observed in the mutants is consistent with damage to bundles of axons at the ONH as a result of increased IOP, creating a pattern of loss that is similarly found in the human condition (Jakobs, Libby et al. 2005). Therefore, not only will researchers have reduced experimental timeframes with our model with RGC loss that mimics the pattern of loss in humans, but also the number of animals needed for examination will be diminished again influencing animal care costs.

The AP-2 β NCC KO mutant model is likely to be useful in a variety of experimental settings to further elucidate the disease process of glaucoma, however it is not without limitations. The corneal phenotype, specifically the corneal opacity that develops due to the deletion of AP-2 β in the NCC population poses a complication as it limits the ability to measure and observe the disease process *in vivo*. Rebound tonometry was used in this study to measure IOP, however this non-invasive method is reliant on the

characteristics of the cornea to calculate IOP. It is possible that the corneal phenotype observed is influencing the measurements recorded, however given the drastic difference in IOP means it is likely that an increase of IOP in the mutants is accurate and due to the closed angle phenotype. However, a more laborious and invasive method of measurement of IOP should be employed to confirm the IOP values – in the mutants versus their wildtype littermates. The corneal opacity also inhibits the examination of the retina and ONH *in vivo* with the use of *in vivo* imaging techniques such as OCT. The ability to use OCT is attractive in a model of glaucoma as it allows researchers to track the progression of the disease within the same mouse over a period of time. However, it should be acknowledged that although these two limitations present further inconvenience they do not nullify AP-2 β NCC KO mutant as a model of glaucoma.

In humans, glaucoma is typically diagnosed due to excavation of the ONH and thinning of the NFL and IPL, the layers that house the nuclei and dendrites of the RGCs respectively (Moura, Raza et al. 2012). The thinning of these layers indicates RGC loss, while the remaining layers of the retina retain their thickness. Thinning of retinal layers other than the NFL and IPL however is not typically a feature of human glaucoma. While the AP-2 β NCC KO mutant model exhibits only thinning of the IPL layer our evidence suggests that both RGCs and dACs are lost at two-months of age which is unlike the human condition. However, it should be noted that other models of glaucoma, including the DBA/2J mice, also experience loss of other retinal cell types and layers (Bayer, Neuhardt et al. 2001, Mao, Hedberg-Buenz et al. 2011, Fernandez-Sanchez, de Sevilla Muller et al. 2014). In addition, the dAC count that in our mutants was only significant at

a relatively high p-value ($P = 0.0225$) when compared to the other statistical significances reached throughout the study. Therefore, it is possible that if we increased the number of NB/DAPI retinal flatmount experiments we would be able to gain a better idea of the difference between dAC in mutants versus wildtypes and if it is a true statistical significance. In addition, it would be prudent to further measure the other retinal layers in older mutants, whether in sections or with confocal microscopy, and compare retinal layer thickness and the numbers of the other retinal cell populations present between mutant and wildtype to confirm if there is in fact a loss of all retinal nuclei.

FUTURE DIRECTIONS AND CONCLUSION

Further work is necessary to fully elucidate the consequences of the deletion of AP-2 β in the NCCs and its effect on the development of anterior eye structures as well as evaluation of the AP-2 β NCC KO mutant as a model of glaucoma. The first area to be addressed is the continued examination of the development of AP-2 β NCC KO mutants past E18.5 to P21. Post-natal stages P0, P4, P7, P14 and P21 would be interesting to observe in order to determine the consequences of loss of AP-2 β expression on structures such as the iris, ciliary body, and trabecular meshwork which continue to develop past birth. These time-points would also allow for the determination of how the closed angle phenotype occurs, whether it is a result of failure of separation between the iris and cornea or due to the lack of corneal endothelium as previously mentioned. Additionally these structures should be analyzed more carefully in adult AP-2 β NCC KO mutants for further detailed characterization of the phenotype. Furthermore, I believe it would be

beneficial to separate the corneal and iridocorneal angle phenotype. This can be done by altering the breeding scheme to include a more specific Cre such as the myocilin Cre that would directly target the trabecular meshwork, or a temporal Cre such as the tamoxifen inducible Wnt1-Cre that would allow the researcher to manipulate the onset of Cre expression. If the tamoxifen inducible Wnt1-Cre was used it would ideally be administered after the cornea has developed around E15.5 to further elucidate AP-2 β 's role in the development of the structures found within the iridocorneal angle. In addition, this may allow for the development of an improved AP-2 β NCC KO model of glaucoma as it may circumvent the corneal phenotype that complicates the model. Lastly, the generation of AP-2 α NCC KO mutants, and potentially AP-2 α/β NCC KO mutants, could be of interest to further elucidate the role of the *Tcfap2* gene in the NCCs that contribute to the POM.

There are also areas of the AP-2 β NCC KO model of glaucoma to be improved upon in order to further prove its validity. Perhaps the most important is developing a time course progression of the disease in order to track the loss of RGCs and the accompanying glaucomatous features. Since the AP-2 β NCC KO mutants display significant loss of RGCs at a relatively young age (two months), all previous experiments should be performed on younger animals (P21) and older animals (6 months) in order to establish the progression of the disease state. In addition, until the corneal phenotype is resolved an invasive method of IOP measurement, such as microneedle cannulation, would be more ideal in order to confirm the increase in IOP of the AP-2 β NCC KO mutants. Measuring the aqueous outflow facility, although challenging, would also assist

in confirming the disruption of aqueous outflow caused by the severe closed angle phenotype of the mutants.

Collectively, this study demonstrates that deletion of AP-2 β from the NCC population resulted in a number of developmental abnormalities of the anterior eye segment that ultimately lead to loss of RGCs. The findings signify the importance of *Tcfap2 β* expression in the POM and eye structures, in addition to implicating it in the developmental network governing the developing anterior segment of the eye. Furthermore, the phenotypes present in the AP-2 β NCC KO mice create an environment conducive to the development of glaucoma suggesting this mutant as a potential model of closed angle glaucoma.

REFERENCES

Aihara, M., J. D. Lindsey and R. N. Weinreb (2003). "Experimental mouse ocular hypertension: establishment of the model." *Invest Ophthalmol Vis Sci* **44**(10): 4314-4320.

Aihara, M., J. D. Lindsey and R. N. Weinreb (2003). "Ocular hypertension in mice with a targeted type I collagen mutation." *Invest Ophthalmol Vis Sci* **44**(4): 1581-1585.

Aliferis, K., C. Stoetzel, V. Pelletier, S. Helle, K. Angioi-Duprez, J. Vigneron, B. Leheup, V. Marion and H. Dollfus (2011). "A novel TFAP2A mutation in familial Branchio-Oculo-Facial Syndrome with predominant ocular phenotype." *Ophthalmic Genet* **32**(4): 250-255.

Anderson, D. R. and A. Hendrickson (1974). "Effect of intraocular pressure on rapid axoplasmic transport in monkey optic nerve." *Invest Ophthalmol* **13**(10): 771-783.

Anderson, M. G., R. S. Smith, N. L. Hawes, A. Zabaleta, B. Chang, J. L. Wiggs and S. W. John (2002). "Mutations in genes encoding melanosomal proteins cause pigmentary glaucoma in DBA/2J mice." *Nat Genet* **30**(1): 81-85.

Araie, M., M. Sekine, Y. Suzuki and N. Koseki (1994). "Factors contributing to the progression of visual field damage in eyes with normal-tension glaucoma." *Ophthalmology* **101**(8): 1440-1444.

Azar, D. T. (2006). "Corneal angiogenic privilege: angiogenic and antiangiogenic factors in corneal avascularity, vasculogenesis, and wound healing (an American Ophthalmological Society thesis)." *Trans Am Ophthalmol Soc* **104**: 264-302.

Bassett, E. A., A. Korol, P. A. Deschamps, R. Buettner, V. A. Wallace, T. Williams and J. A. West-Mays (2012). "Overlapping expression patterns and redundant roles for AP-2 transcription factors in the developing mammalian retina." *Dev Dyn* **241**(4): 814-829.

Bassett, E. A., G. F. Pontoriero, W. Feng, T. Marquardt, M. E. Fini, T. Williams and J. A. West-Mays (2007). "Conditional deletion of activating protein 2alpha (AP-2alpha) in the developing retina demonstrates non-cell-autonomous roles for AP-2alpha in optic cup development." *Mol Cell Biol* **27**(21): 7497-7510.

Bayer, A. U., T. Neuhardt, A. C. May, P. Martus, K. P. Maag, S. Brodie, E. Lutjen-Drecoll, S. M. Podos and T. Mittag (2001). "Retinal morphology and ERG response in the DBA/2Nnia mouse model of angle-closure glaucoma." *Invest Ophthalmol Vis Sci* **42**(6): 1258-1265.

Bjorklund, H., A. Bignami and D. Dahl (1985). "Immunohistochemical demonstration of glial fibrillary acidic protein in normal rat Muller glia and retinal astrocytes." *Neurosci Lett* **54**(2-3): 363-368.

Boland, M. V. and H. A. Quigley (2007). "Risk factors and open-angle glaucoma: classification and application." J Glaucoma **16**(4): 406-418.

Bosher, J. M., N. F. Totty, J. J. Hsuan, T. Williams and H. C. Hurst (1996). "A family of AP-2 proteins regulates c-erbB-2 expression in mammary carcinoma." Oncogene **13**(8): 1701-1707.

Brewer, S., W. Feng, J. Huang, S. Sullivan and T. Williams (2004). "Wnt1-Cre-mediated deletion of AP-2alpha causes multiple neural crest-related defects." Dev Biol **267**(1): 135-152.

Chang, E. E. and J. L. Goldberg (2012). "Glaucoma 2.0: neuroprotection, neuroregeneration, neuroenhancement." Ophthalmology **119**(5): 979-986.

Chatterjee, A., D. J. Oh, M. H. Kang and D. J. Rhee (2013). "Central corneal thickness does not correlate with TonoLab-measured IOP in several mouse strains with single transgenic mutations of matricellular proteins." Exp Eye Res **115**: 106-112.

Chow, R. L. and R. A. Lang (2001). "Early eye development in vertebrates." Annu Rev Cell Dev Biol **17**: 255-296.

CNIB, a. t. C. O. S. (2011). "The cost of vision loss in Canada." Access Economics Pty Limited: 1-115.

Coleman, A. L. and S. Miglior (2008). "Risk factors for glaucoma onset and progression." Surv Ophthalmol **53 Suppl1**: S3-10.

Cvekl, A. and E. R. Tamm (2004). "Anterior eye development and ocular mesenchyme: new insights from mouse models and human diseases." Bioessays **26**(4): 374-386.

Danielian, P. S., D. Muccino, D. H. Rowitch, S. K. Michael and A. P. McMahon (1998). "Modification of gene activity in mouse embryos in utero by a tamoxifen-inducible form of Cre recombinase." Curr Biol **8**(24): 1323-1326.

Ding, C., P. Wang and N. Tian (2011). "Effect of general anesthetics on IOP in elevated IOP mouse model." Exp Eye Res **92**(6): 512-520.

Dreyer, E. B. and S. A. Lipton (1999). "New perspectives on glaucoma." JAMA **281**(4): 306-308.

Eckert, D., S. Buhl, S. Weber, R. Jager and H. Schorle (2005). "The AP-2 family of transcription factors." Genome Biol **6**(13): 246.

Ellenberg, D., D. T. Azar, J. A. Hallak, F. Tobaigy, K. Y. Han, S. Jain, Z. Zhou and J. H. Chang (2010). "Novel aspects of corneal angiogenic and lymphangiogenic privilege." Prog Retin Eye Res **29**(3): 208-248.

Evans, A. L. and P. J. Gage (2005). "Expression of the homeobox gene Pitx2 in neural crest is required for optic stalk and ocular anterior segment development." Hum Mol Genet **14**(22): 3347-3359.

Fernandez-Sanchez, L., L. P. de Sevilla Muller, N. C. Brecha and N. Cuenca (2014). "Loss of outer retinal neurons and circuitry alterations in the DBA/2J mouse." Invest Ophthalmol Vis Sci **55**(9): 6059-6072.

Friedman, D. S., R. C. Wolfs, B. J. O'Colmain, B. E. Klein, H. R. Taylor, S. West, M. C. Leske, P. Mitchell, N. Congdon, J. Kempen and G. Eye Diseases Prevalence Research (2004). "Prevalence of open-angle glaucoma among adults in the United States." Arch Ophthalmol **122**(4): 532-538.

Gage, P. J., C. Kuang and A. L. Zacharias (2014). "The homeodomain transcription factor PITX2 is required for specifying correct cell fates and establishing angiogenic privilege in the developing cornea." Dev Dyn **243**(11): 1391-1400.

Gage, P. J., W. Rhoades, S. K. Prucka and T. Hjalt (2005). "Fate maps of neural crest and mesoderm in the mammalian eye." Invest Ophthalmol Vis Sci **46**(11): 4200-4208.

Gage, P. J., H. Suh and S. A. Camper (1999). "Dosage requirement of Pitx2 for development of multiple organs." Development **126**(20): 4643-4651.

Gammill, L. S. and M. Bronner-Fraser (2003). "Neural crest specification: migrating into genomics." Nat Rev Neurosci **4**(10): 795-805.

Gilbert, S. F. (2006). Development of the Vertebrate Eye. Sunderland (MA), Sinauer Associates.

Gould, D. B. and S. W. John (2002). "Anterior segment dysgenesis and the developmental glaucomas are complex traits." Hum Mol Genet **11**(10): 1185-1193.

Gould, D. B., R. S. Smith and S. W. John (2004). "Anterior segment development relevant to glaucoma." Int J Dev Biol **48**(8-9): 1015-1029.

Graw, J. (1996). "Genetic aspects of embryonic eye development in vertebrates." Dev Genet **18**(3): 181-197.

Haustein, J. (1983). "On the ultrastructure of the developing and adult mouse corneal stroma." Anat Embryol (Berl) **168**(2): 291-305.

Heffner, C. S., C. Herbert Pratt, R. P. Babiuk, Y. Sharma, S. F. Rockwood, L. R. Donahue, J. T. Eppig and S. A. Murray (2012). "Supporting conditional mouse mutagenesis with a comprehensive cre characterization resource." Nat Commun **3**: 1218.

Hilger-Eversheim, K., M. Moser, H. Schorle and R. Buettner (2000). "Regulatory roles of AP-2 transcription factors in vertebrate development, apoptosis and cell-cycle control." Gene **260**(1-2): 1-12.

Idrees, F., D. Vaideanu, S. G. Fraser, J. C. Sowden and P. T. Khaw (2006). "A review of anterior segment dysgeneses." Surv Ophthalmol **51**(3): 213-231.

Jakobs, T. C., R. T. Libby, Y. Ben, S. W. John and R. H. Masland (2005). "Retinal ganglion cell degeneration is topological but not cell type specific in DBA/2J mice." J Cell Biol **171**(2): 313-325.

Jeon, C. J., E. Strettoi and R. H. Masland (1998). "The major cell populations of the mouse retina." J Neurosci **18**(21): 8936-8946.

John, S. W., R. S. Smith, O. V. Savinova, N. L. Hawes, B. Chang, D. Turnbull, M. Davisson, T. H. Roderick and J. R. Heckenlively (1998). "Essential iris atrophy, pigment dispersion, and glaucoma in DBA/2J mice." Invest Ophthalmol Vis Sci **39**(6): 951-962.

Johnston, M. C., D. M. Noden, R. D. Hazelton, J. L. Coulombre and A. J. Coulombre (1979). "Origins of avian ocular and periocular tissues." Exp Eye Res **29**(1): 27-43.

Ju, W. K., K. Y. Kim, J. D. Lindsey, M. Angert, K. X. Duong-Polk, R. T. Scott, J. J. Kim, I. Kukhmazov, M. H. Ellisman, G. A. Perkins and R. N. Weinreb (2008). "Intraocular pressure elevation induces mitochondrial fission and triggers OPA1 release in glaucomatous optic nerve." Invest Ophthalmol Vis Sci **49**(11): 4903-4911.

Kidson, S. H., T. Kume, K. Deng, V. Winfrey and B. L. Hogan (1999). "The forkhead/winged-helix gene, *Mfl*, is necessary for the normal development of the cornea and formation of the anterior chamber in the mouse eye." Dev Biol **211**(2): 306-322.

Kipfer-Kauer, A., S. J. McKinnon, B. E. Frueh and D. Goldblum (2010). "Distribution of amyloid precursor protein and amyloid-beta in ocular hypertensive C57BL/6 mouse eyes." Curr Eye Res **35**(9): 828-834.

Knoers, N. V., E. M. Bongers, S. E. van Beersum, E. J. Lommen, H. van Bokhoven and F. A. Hol (2000). "Nail-patella syndrome: identification of mutations in the *LMX1B* gene in Dutch families." J Am Soc Nephrol **11**(9): 1762-1766.

Kolko (2015). "Present and New Treatment Strategies in the Management of Glaucoma." Open Ophthalmol J **9**: 89-100.

Kume, T., K. Y. Deng, V. Winfrey, D. B. Gould, M. A. Walter and B. L. Hogan (1998). "The forkhead/winged helix gene *Mf1* is disrupted in the pleiotropic mouse mutation congenital hydrocephalus." Cell **93**(6): 985-996.

Kupfer, C. and M. I. Kaiser-Kupfer (1978). "New hypothesis of developmental anomalies of the anterior chamber associated with glaucoma." Trans Ophthalmol Soc U K **98**(2): 213-215.

Kupfer, C. and M. I. Kaiser-Kupfer (1979). "Observations on the development of the anterior chamber angle with reference to the pathogenesis of congenital glaucomas." Am J Ophthalmol **88**(3 Pt 1): 424-426.

Lampert, P. W., M. H. Vogel and L. E. Zimmerman (1968). "Pathology of the optic nerve in experimental acute glaucoma. Electron microscopic studies." Invest Ophthalmol **7**(2): 199-213.

Libby, R. T., M. G. Anderson, I. H. Pang, Z. H. Robinson, O. V. Savinova, I. M. Cosma, A. Snow, L. A. Wilson, R. S. Smith, A. F. Clark and S. W. John (2005). "Inherited glaucoma in DBA/2J mice: pertinent disease features for studying the neurodegeneration." Vis Neurosci **22**(5): 637-648.

Lichter, P. R., J. E. Richards, C. A. Downs, H. M. Stringham, M. Boehnke and F. A. Farley (1997). "Cosegregation of open-angle glaucoma and the nail-patella syndrome." Am J Ophthalmol **124**(4): 506-515.

Lindsey, J. D. and R. N. Weinreb (2002). "Identification of the mouse uveoscleral outflow pathway using fluorescent dextran." Invest Ophthalmol Vis Sci **43**(7): 2201-2205.

Lines, M. A., K. Kozlowski and M. A. Walter (2002). "Molecular genetics of Axenfeld-Rieger malformations." Hum Mol Genet **11**(10): 1177-1184.

Lu, M. F., C. Pressman, R. Dyer, R. L. Johnson and J. F. Martin (1999). "Function of Rieger syndrome gene in left-right asymmetry and craniofacial development." Nature **401**(6750): 276-278.

Luo, T., Y. H. Lee, J. P. Saint-Jeannet and T. D. Sargent (2003). "Induction of neural crest in *Xenopus* by transcription factor AP2alpha." Proc Natl Acad Sci U S A **100**(2): 532-537.

Mao, M., A. Hedberg-Buenz, D. Koehn, S. W. John and M. G. Anderson (2011). "Anterior segment dysgenesis and early-onset glaucoma in *nee* mice with mutation of *Sh3pxd2b*." Invest Ophthalmol Vis Sci **52**(5): 2679-2688.

McKinnon, S. J., C. L. Schlamp and R. W. Nickells (2009). "Mouse models of retinal ganglion cell death and glaucoma." *Exp Eye Res* **88**(4): 816-824.

Mears, A. J., F. Mirzayans, D. B. Gould, W. G. Pearce and M. A. Walter (1996). "Autosomal dominant iridogoniodysgenesis anomaly maps to 6p25." *Am J Hum Genet* **59**(6): 1321-1327.

Milunsky, J. M., T. A. Maher, G. Zhao, A. E. Roberts, H. J. Stalker, R. T. Zori, M. N. Burch, M. Clemens, J. B. Mulliken, R. Smith and A. E. Lin (2008). "TFAP2A mutations result in branchio-oculo-facial syndrome." *Am J Hum Genet* **82**(5): 1171-1177.

Milunsky, J. M., T. M. Maher, G. Zhao, Z. Wang, J. B. Mulliken, D. Chitayat, M. Clemens, H. J. Stalker, M. Bauer, M. Burch, S. Chenier, M. L. Cunningham, A. V. Drack, S. Janssens, A. Karlea, R. Klatt, U. Kini, O. Klein, A. M. Lachmeijer, A. Megarbane, N. J. Mendelsohn, W. S. Meschino, G. R. Mortier, S. Parkash, C. R. Ray, A. Roberts, A. Roberts, W. Reardon, R. E. Schnur, R. Smith, M. Splitt, K. Tezcan, M. L. Whiteford, D. A. Wong, R. Zori and A. E. Lin (2011). "Genotype-phenotype analysis of the branchio-oculo-facial syndrome." *Am J Med Genet A* **155A**(1): 22-32.

Minckler, D. S., A. H. Bunt and G. W. Johanson (1977). "Orthograde and retrograde axoplasmic transport during acute ocular hypertension in the monkey." *Invest Ophthalmol Vis Sci* **16**(5): 426-441.

Mitchell, P. J., P. M. Timmons, J. M. Hebert, P. W. Rigby and R. Tjian (1991). "Transcription factor AP-2 is expressed in neural crest cell lineages during mouse embryogenesis." *Genes Dev* **5**(1): 105-119.

Mohibullah, N., A. Donner, J. A. Ippolito and T. Williams (1999). "SELEX and missing phosphate contact analyses reveal flexibility within the AP-2[alpha] protein: DNA binding complex." *Nucleic Acids Res* **27**(13): 2760-2769.

Moser, M., A. Imhof, A. Pscherer, R. Bauer, W. Amselgruber, F. Sinowatz, F. Hofstadter, R. Schule and R. Buettner (1995). "Cloning and characterization of a second AP-2 transcription factor: AP-2 beta." *Development* **121**(9): 2779-2788.

Moser, M., A. Pscherer, C. Roth, J. Becker, G. Mucher, K. Zerres, C. Dixkens, J. Weis, L. Guay-Woodford, R. Buettner and R. Fassler (1997). "Enhanced apoptotic cell death of renal epithelial cells in mice lacking transcription factor AP-2beta." *Genes Dev* **11**(15): 1938-1948.

Moser, M., J. Ruschhoff and R. Buettner (1997). "Comparative analysis of AP-2 alpha and AP-2 beta gene expression during murine embryogenesis." *Dev Dyn* **208**(1): 115-124.

Moura, A. L., A. S. Raza, M. A. Lazow, C. G. De Moraes and D. C. Hood (2012). "Retinal ganglion cell and inner plexiform layer thickness measurements in regions of

severe visual field sensitivity loss in patients with glaucoma." Eye (Lond) **26**(9): 1188-1193.

Nadal-Nicolas, F. M., M. Jimenez-Lopez, P. Sobrado-Calvo, L. Nieto-Lopez, I. Canovas-Martinez, M. Salinas-Navarro, M. Vidal-Sanz and M. Agudo (2009). "Brn3a as a marker of retinal ganglion cells: qualitative and quantitative time course studies in naive and optic nerve-injured retinas." Invest Ophthalmol Vis Sci **50**(8): 3860-3868.

Neufeld, A. H., M. R. Hernandez and M. Gonzalez (1997). "Nitric oxide synthase in the human glaucomatous optic nerve head." Arch Ophthalmol **115**(4): 497-503.

Pang, J. J. and S. M. Wu (2011). "Morphology and immunoreactivity of retrogradely double-labeled ganglion cells in the mouse retina." Invest Ophthalmol Vis Sci **52**(7): 4886-4896.

Pease, M. E., S. J. McKinnon, H. A. Quigley, L. A. Kerrigan-Baumrind and D. J. Zack (2000). "Obstructed axonal transport of BDNF and its receptor TrkB in experimental glaucoma." Invest Ophthalmol Vis Sci **41**(3): 764-774.

Pei, Y. F. and J. A. Rhodin (1970). "The prenatal development of the mouse eye." Anat Rec **168**(1): 105-125.

Pei, Y. F. and J. A. Rhodin (1971). "Electron microscopic study of the development of the mouse corneal epithelium." Invest Ophthalmol **10**(11): 811-825.

Perveen, R., I. C. Lloyd, J. Clayton-Smith, A. Churchill, V. van Heyningen, I. Hanson, D. Taylor, C. McKeown, M. Super, B. Kerr, R. Winter and G. C. Black (2000). "Phenotypic variability and asymmetry of Rieger syndrome associated with PITX2 mutations." Invest Ophthalmol Vis Sci **41**(9): 2456-2460.

Pontoriero, G. F., P. Deschamps, R. Ashery-Padan, R. Wong, Y. Yang, J. Zavadil, A. Cvekl, S. Sullivan, T. Williams and J. A. West-Mays (2008). "Cell autonomous roles for AP-2alpha in lens vesicle separation and maintenance of the lens epithelial cell phenotype." Dev Dyn **237**(3): 602-617.

Pressman, C. L., H. Chen and R. L. Johnson (2000). "LMX1B, a LIM homeodomain class transcription factor, is necessary for normal development of multiple tissues in the anterior segment of the murine eye." Genesis **26**(1): 15-25.

Quigley, H. and D. R. Anderson (1976). "The dynamics and location of axonal transport blockade by acute intraocular pressure elevation in primate optic nerve." Invest Ophthalmol **15**(8): 606-616.

Quigley, H. A. and A. T. Broman (2006). "The number of people with glaucoma worldwide in 2010 and 2020." Br J Ophthalmol **90**(3): 262-267.

- Reneker, L. W., D. W. Silversides, L. Xu and P. A. Overbeek (2000). "Formation of corneal endothelium is essential for anterior segment development - a transgenic mouse model of anterior segment dysgenesis." Development **127**(3): 533-542.
- Ruiz-Ederra, J. and A. S. Verkman (2006). "Mouse model of sustained elevation in intraocular pressure produced by episcleral vein occlusion." Exp Eye Res **82**(5): 879-884.
- Sappington, R. M., B. J. Carlson, S. D. Crish and D. J. Calkins (2010). "The microbead occlusion model: a paradigm for induced ocular hypertension in rats and mice." Invest Ophthalmol Vis Sci **51**(1): 207-216.
- Sarthy, P. V., M. Fu and J. Huang (1991). "Developmental expression of the glial fibrillary acidic protein (GFAP) gene in the mouse retina." Cell Mol Neurobiol **11**(6): 623-637.
- Satoda, M., M. E. Pierpont, G. A. Diaz, R. A. Bornemeier and B. D. Gelb (1999). "Char syndrome, an inherited disorder with patent ductus arteriosus, maps to chromosome 6p12-p21." Circulation **99**(23): 3036-3042.
- Satoda, M., F. Zhao, G. A. Diaz, J. Burn, J. Goodship, H. R. Davidson, M. E. Pierpont and B. D. Gelb (2000). "Mutations in TFAP2B cause Char syndrome, a familial form of patent ductus arteriosus." Nat Genet **25**(1): 42-46.
- Schorle, H., P. Meier, M. Buchert, R. Jaenisch and P. J. Mitchell (1996). "Transcription factor AP-2 essential for cranial closure and craniofacial development." Nature **381**(6579): 235-238.
- Senatorov, V., I. Malyukova, R. Fariss, E. F. Wawrousek, S. Swaminathan, S. K. Sharan and S. Tomarev (2006). "Expression of mutated mouse myocilin induces open-angle glaucoma in transgenic mice." J Neurosci **26**(46): 11903-11914.
- Seo, S., H. P. Singh, P. M. Laca, A. Sasman, A. Fatima, T. Liu, K. M. Schultz, D. W. Losordo, O. J. Lehmann and T. Kume (2012). "Forkhead box transcription factor FoxC1 preserves corneal transparency by regulating vascular growth." Proc Natl Acad Sci U S A **109**(6): 2015-2020.
- Serbedzija, G. N., M. Bronner-Fraser and S. E. Fraser (1994). "Developmental potential of trunk neural crest cells in the mouse." Development **120**(7): 1709-1718.
- Shields, M. B. (1987). "A common pathway for developmental glaucomas." Trans Am Ophthalmol Soc **85**: 222-237.
- Shimazawa, M., Y. Inokuchi, Y. Ito, H. Murata, M. Aihara, M. Miura, M. Araie and H. Hara (2007). "Involvement of ER stress in retinal cell death." Mol Vis **13**: 578-587.

Smith, R. S., A. Zabaleta, T. Kume, O. V. Savinova, S. H. Kidson, J. E. Martin, D. Y. Nishimura, W. L. Alward, B. L. Hogan and S. W. John (2000). "Haploinsufficiency of the transcription factors FOXC1 and FOXC2 results in aberrant ocular development." Hum Mol Genet **9**(7): 1021-1032.

Smith, R. S., A. Zabaleta, O. V. Savinova and S. W. John (2001). "The mouse anterior chamber angle and trabecular meshwork develop without cell death." BMC Dev Biol **1**: 3.

Stoetzel, C., S. Riehm, V. Bennouna Greene, V. Pelletier, J. Vigneron, B. Leheup, V. Marion, S. Helle, J. M. Danse, C. Thibault, L. Moulinier, F. Veillon and H. Dollfus (2009). "Confirmation of TFAP2A gene involvement in branchio-oculo-facial syndrome (BOFS) and report of temporal bone anomalies." Am J Med Genet A **149A**(10): 2141-2146.

Tanihara, H., M. Hangai, S. Sawaguchi, H. Abe, M. Kageyama, F. Nakazawa, E. Shirasawa and Y. Honda (1997). "Up-regulation of glial fibrillary acidic protein in the retina of primate eyes with experimental glaucoma." Arch Ophthalmol **115**(6): 752-756.

Tham, Y. C., X. Li, T. Y. Wong, H. A. Quigley, T. Aung and C. Y. Cheng (2014). "Global prevalence of glaucoma and projections of glaucoma burden through 2040: a systematic review and meta-analysis." Ophthalmology **121**(11): 2081-2090.

Tumer, Z. and D. Bach-Holm (2009). "Axenfeld-Rieger syndrome and spectrum of PITX2 and FOXC1 mutations." Eur J Hum Genet **17**(12): 1527-1539.

Varma, R., M. Ying-Lai, B. A. Francis, B. B. Nguyen, J. Deneen, M. R. Wilson, S. P. Azen and G. Los Angeles Latino Eye Study (2004). "Prevalence of open-angle glaucoma and ocular hypertension in Latinos: the Los Angeles Latino Eye Study." Ophthalmology **111**(8): 1439-1448.

Vassilev, V. S., M. Mandai, S. Yonemura and M. Takeichi (2012). "Loss of N-cadherin from the endothelium causes stromal edema and epithelial dysgenesis in the mouse cornea." Invest Ophthalmol Vis Sci **53**(11): 7183-7193.

Wang, S. W., X. Mu, W. J. Bowers, D. S. Kim, D. J. Plas, M. C. Crair, H. J. Federoff, L. Gan and W. H. Klein (2002). "Brn3b/Brn3c double knockout mice reveal an unsuspected role for Brn3c in retinal ganglion cell axon outgrowth." Development **129**(2): 467-477.

Wang, X., S. S.-W. Tay and Y.-K. Ng (2000). "An immunohistochemical study of neuronal and glial cell reactions in retinæ of rats with experimental glaucoma." Experimental Brain Research **132**(4): 476-484.

Waring, G. O., 3rd, W. M. Bourne, H. F. Edelhauser and K. R. Kenyon (1982). "The corneal endothelium. Normal and pathologic structure and function." Ophthalmology **89**(6): 531-590.

West-Mays, J. A., J. Zhang, T. Nottoli, S. Hagopian-Donaldson, D. Libby, K. J. Strissel and T. Williams (1999). "AP-2alpha transcription factor is required for early morphogenesis of the lens vesicle." Dev Biol **206**(1): 46-62.

Zhang, J., S. Hagopian-Donaldson, G. Serbedzija, J. Elsemore, D. Plehn-Dujowich, A. P. McMahon, R. A. Flavell and T. Williams (1996). "Neural tube, skeletal and body wall defects in mice lacking transcription factor AP-2." Nature **381**(6579): 238-241.

Zhao, F., C. G. Weismann, M. Satoda, M. E. Pierpont, E. Sweeney, E. M. Thompson and B. D. Gelb (2001). "Novel TFAP2B mutations that cause Char syndrome provide a genotype-phenotype correlation." Am J Hum Genet **69**(4): 695-703.

FIGURES

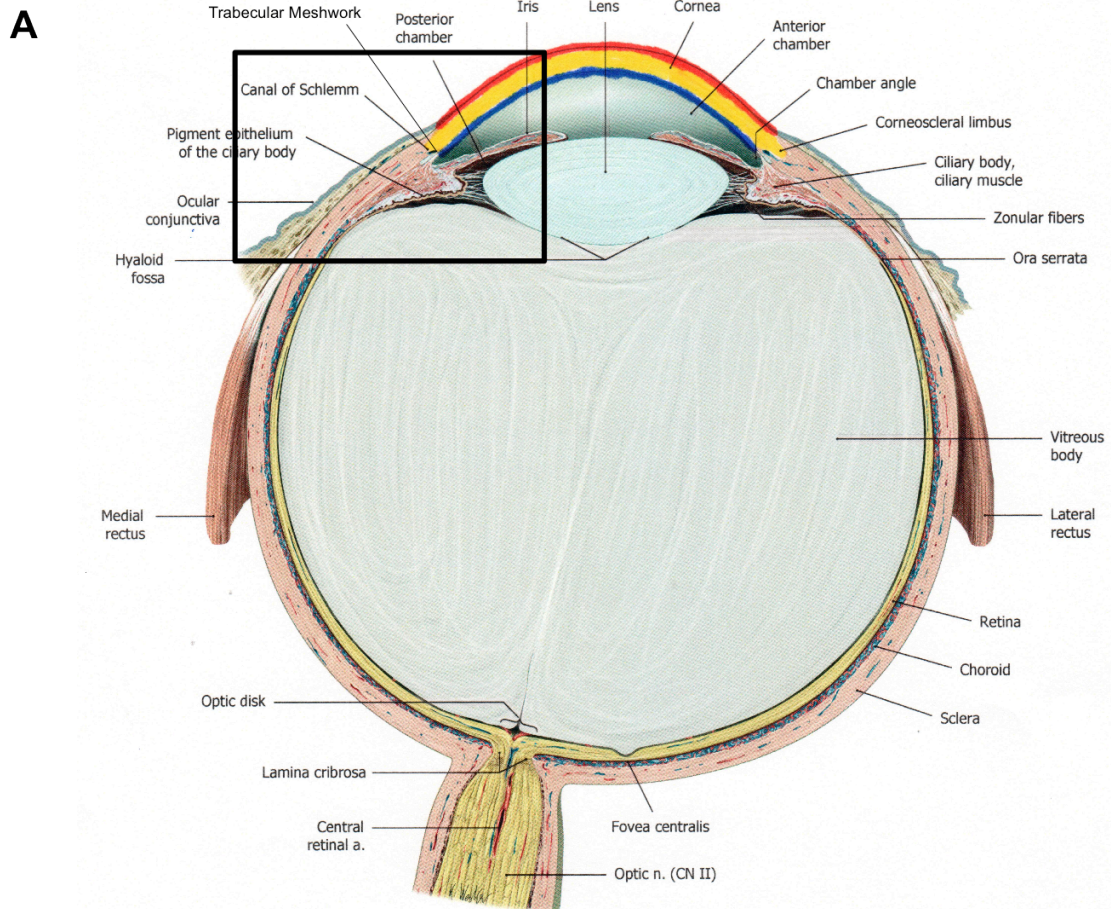


Figure 1. General Anatomy of the Eye. (A) A schematic depicting the anatomical structures of the mammalian eye. The area within the square is magnified in B. **(B)** The green arrow traces the pathway of aqueous humour as it is produced by the ciliary body, travels between the lens and the iris to enter the anterior chamber and continues to the iridocorneal angle where it will drain out of the Trabecular Meshwork and Schlemm’s canal or the Uveoscleral Pathway (Aqua arrow). In the event that either of these pathways are disrupted, an increase in IOP is caused that could lead to glaucomatous features (Adapted from Thieme Atlas of Anatomy, Second Edition, 2015).

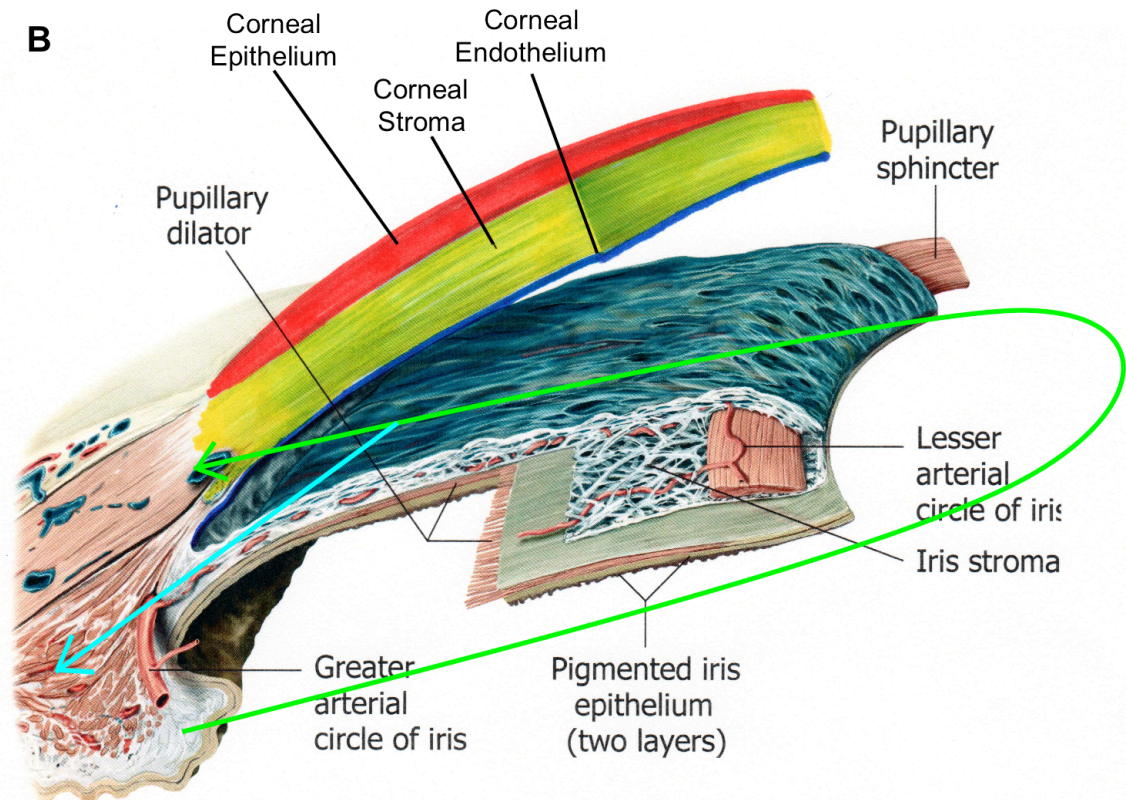


Figure 1. General Anatomy of the Eye. (A) A schematic depicting the anatomical structures of the mammalian eye. The area within the square is magnified in B. **(B)** The green arrow traces the pathway of aqueous humour as it is produced by the ciliary body, travels between the lens and the iris to enter the anterior chamber and continues to the iridocorneal angle where it will drain out of the Trabecular Meshwork and Schlemm's canal or the Uveoscleral Pathway (Aqua arrow). In the event that either of these pathways are disrupted, an increase in IOP is caused that could lead to glaucomatous features (Adapted from Thieme Atlas of Anatomy, Second Edition, 2015).

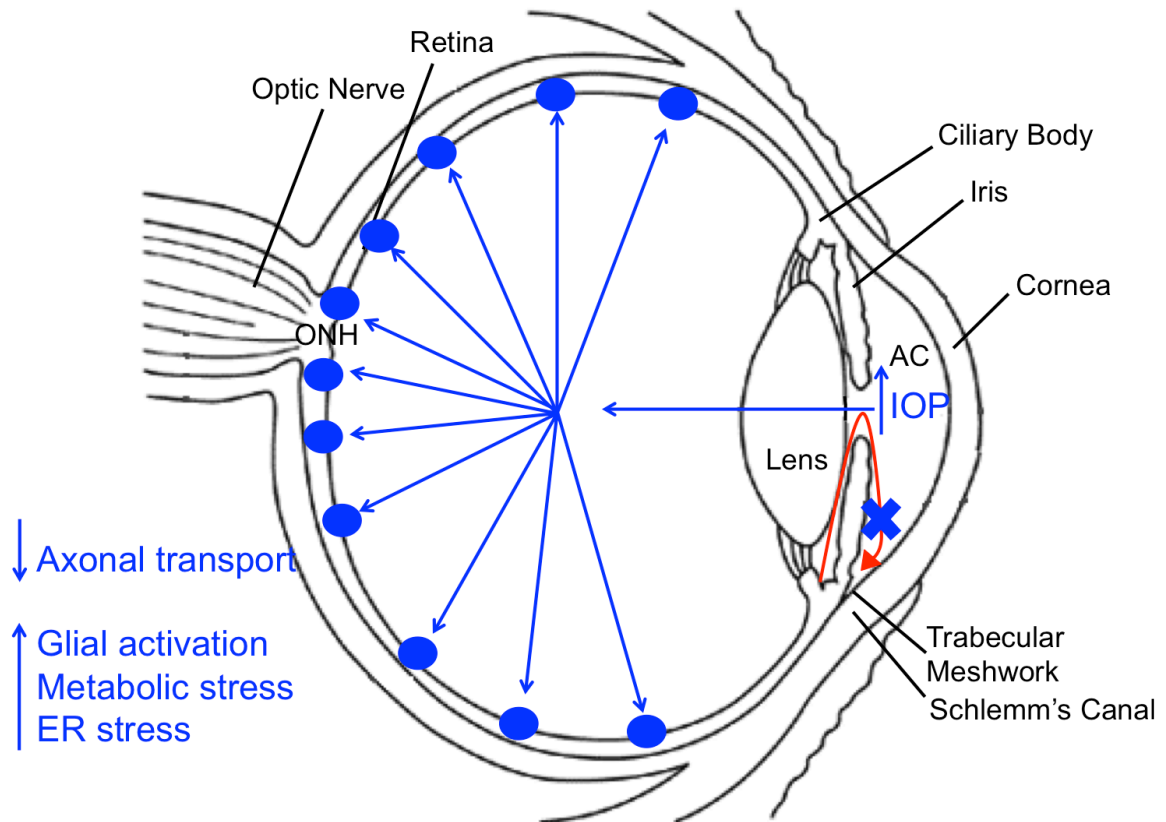


Figure 2. Schematic depicting theories of the relationship between increased IOP and the development of glaucoma. When an impediment of the aqueous outflow pathway (red arrow) occurs (blue X) the pressure within the anterior chamber increases, also known as increased IOP. This increased pressure translates to the back of the eye where it will exert itself upon the retina, particularly at the optic nerve head (ONH). As a result it is thought that axonal transport of trophic factors is decreased, and/or there is an increase of glial activation, metabolic and ER stress.

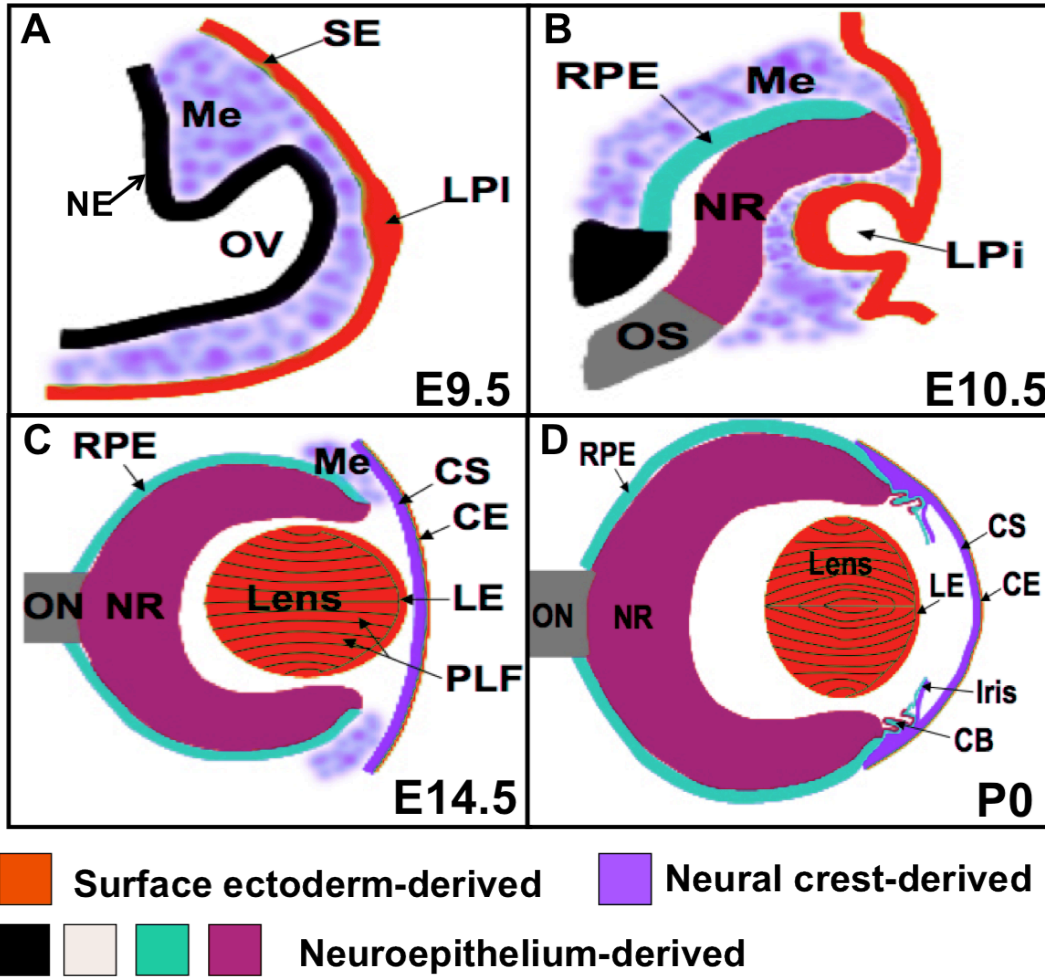


Figure 3. Vertebrate eye development and tissue derivations. (A) Formation of the optic vesicle occurs as the neuroepithelium (NE, black) of the diencephalon evaginates, moving through the periocular mesenchyme (Me, purple) until it reaches the surface ectoderm (SE, red) forming the optic vesicle (OV) which will induce formation of the lens placode (LPI). (B) The OV will invaginate along with the thickened surface ectoderm that will form the lens pit (LPi) (OS; optic stalk). (C) The LPi will detach to form the lens vesicle and ultimately the lens. The overlying surface ectoderm will then differentiate to form the future corneal epithelium (CE, red) and the Me will have migrated between the surface ectoderm and lens to give rise to the corneal stroma (CS) and endothelium (CE). The optic cup will differentiate into the neural retina (NR) and the retinal pigmented epithelium (RPE) (LE; lens epithelium, PLF; proliferating lens fibers). (D) The CS and CE are derived from the migrating Me (purple). The anterior rim of the optic cup will give rise to the epithelia of both the iris (aqua) and the ciliary body (CB, aqua). The Me forms the iris stroma (purple), and muscle and stroma of the ciliary body (CB, purple) (Adapted from Bassett, E.A, 2012).

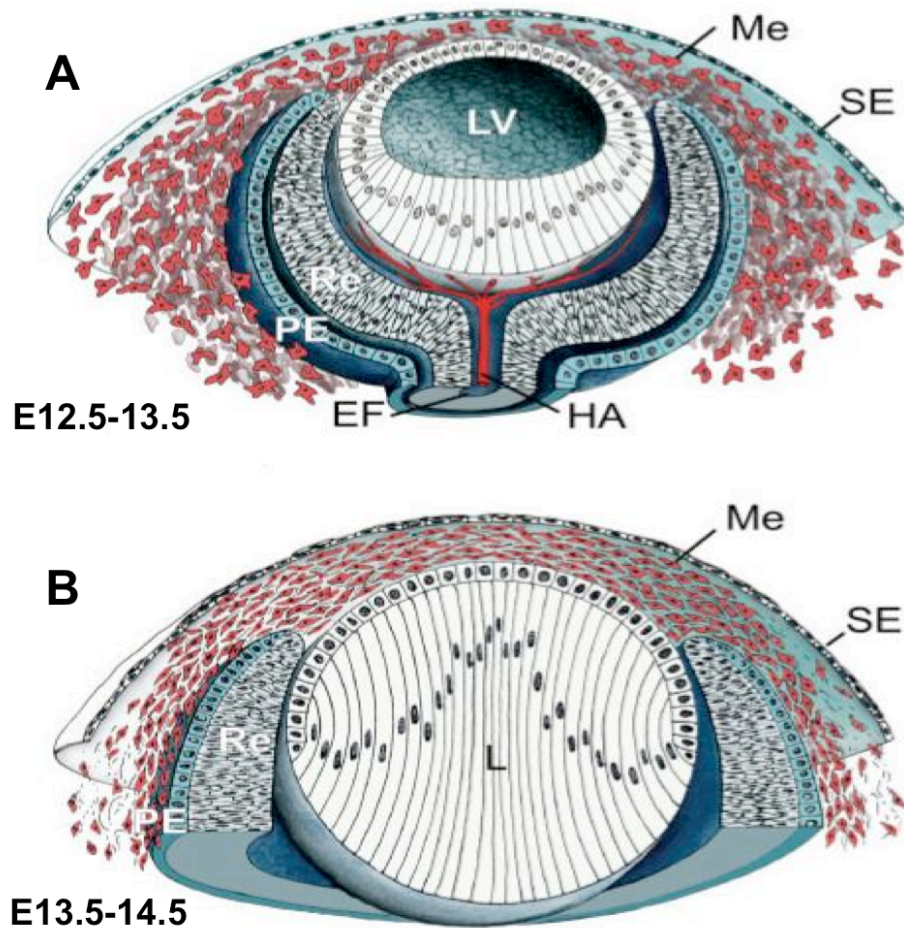


Figure 4. Migration of the POM in the mouse eye and development of the anterior segment. (A) Once the lens vesicle (LV) has detached from the surface ectoderm (SE) the space between the two structures will be filled with migrating mesenchymal cells (Me) (Re; neural retina, PE; retinal pigmented epithelium, HA; hyaloid artery, EF; embryonic (choroidal) fissure). (B) Several flat layers of condensed mesenchymal cells are formed and separated by loose fibrillar extracellular matrix. (C) The mesenchymal cells closest to the lens will flatten and form the corneal endothelium (CEn), the overlying surface ectoderm will differentiate into the corneal epithelium (CEp), and the mesenchyme found between these structures will differentiate into the corneal stroma (CS). A second wave of mesenchymal cells will arrive at the angle between the future cornea and the anterior rim of the optic cup (Me). (D) The anterior rim of the optic cup will give rise to form the epithelia of the iris and ciliary body while the second wave of mesenchymal cells will migrate alongside to differentiate into the stroma of both structures (SIr; stroma of the iris, SCB; stroma of the ciliary body, AC; anterior chamber) (Adapted from Cvekl, A. et al., 2004).

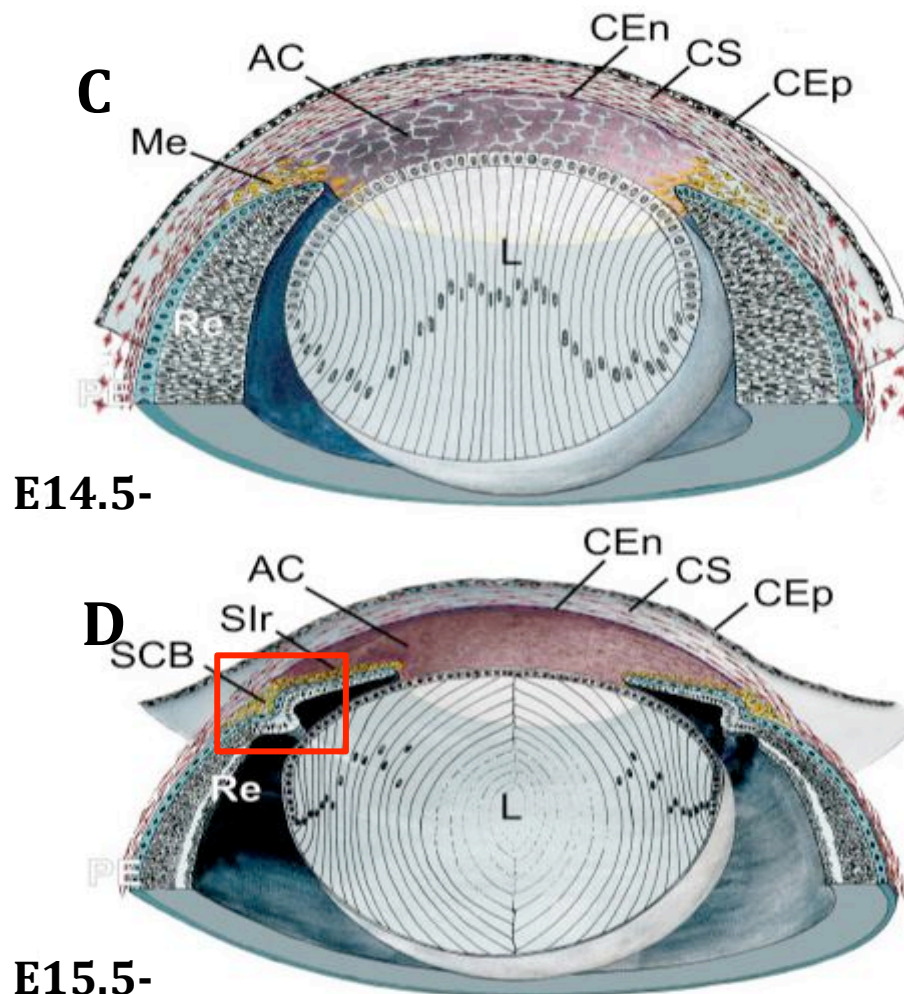


Figure 4. Migration of the POM in the mouse eye and development of the anterior segment. (A) Once the lens vesicle (LV) has detached from the surface ectoderm (SE) the space between the two structures will be filled with migrating mesenchymal cells (Me) (Re; neural retina, PE; retinal pigmented epithelium, HA; hyaloid artery, EF; embryonic (choroidal) fissure). (B) Several flat layers of condensed mesenchymal cells are formed and separated by loose fibrillar extracellular matrix. (C) The mesenchymal cells closest to the lens will flatten and form the corneal endothelium (CEn), the overlying surface ectoderm will differentiate into the corneal epithelium (CEp), and the mesenchyme found between these structures will differentiate into the corneal stroma (CS). A second wave of mesenchymal cells will arrive at the angle between the future cornea and the anterior rim of the optic cup (Me). (D) The anterior rim of the optic cup will give rise to form the epithelia of the iris and ciliary body while the second wave of mesenchymal cells will migrate alongside to differentiate in the stroma of both structures (Slr; stroma of the iris, SCB; stroma of the ciliary body, AC; anterior chamber) (Adapted from Cvekl, A. et al., 2004).

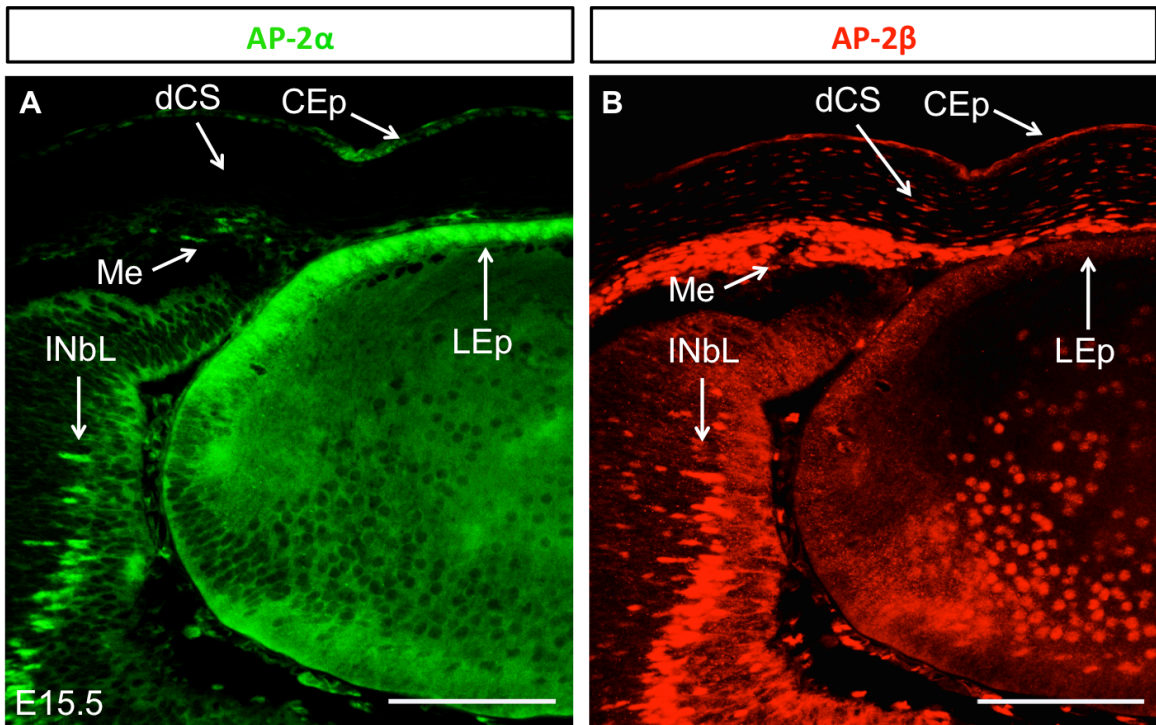


Figure 5. The expression of AP-2 α and AP-2 β in an E15.5 murine eye. (A) AP-2 α is expressed at the lens epithelium (LEp), corneal epithelium (CEp) and the inner neuroblast layer (INbL) of the developing retina. **(B)** AP-2 β is also expressed in the CEp, the developing corneal stroma (CS) and the INbL, and importantly is strongly expressed in the periocular mesenchyme (Me). Scalebars set to 100 μ m.

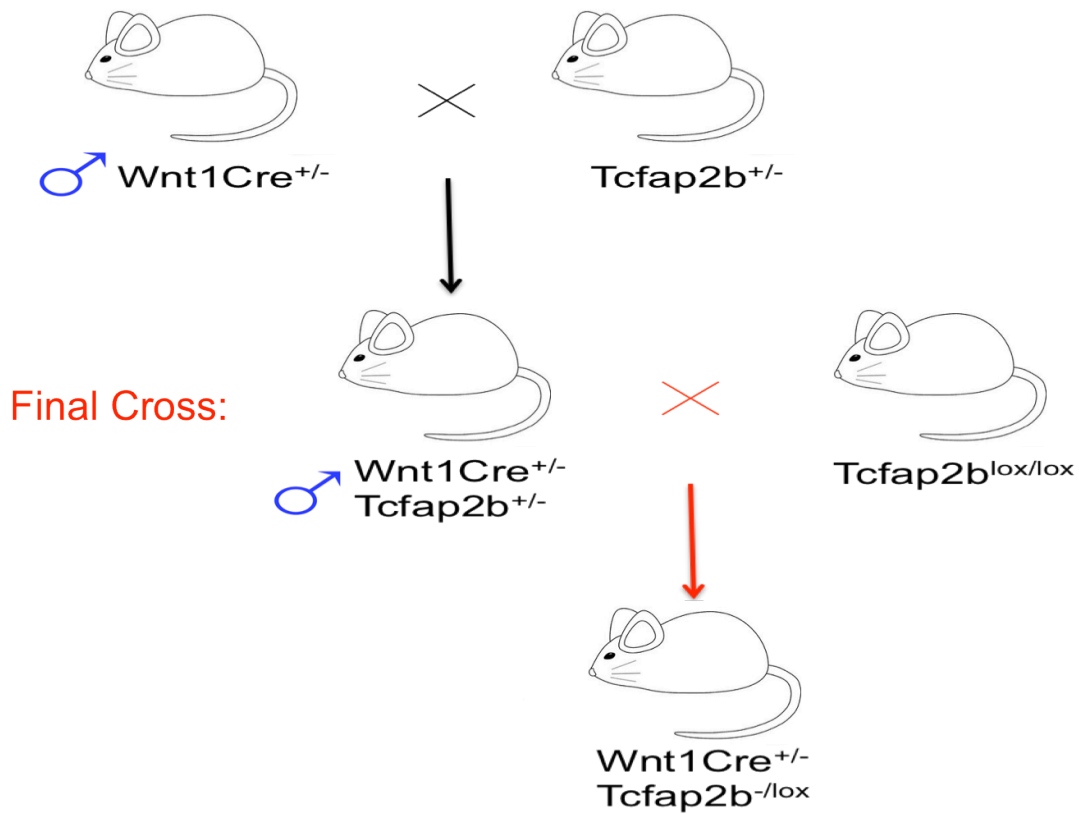


Figure 6. Generation of AP-2 β NCC KO mutants. Mice heterozygous for the *Tcfap2 β* null allele are crossed with male heterozygous *Cre*^{+/-} transgenic mice that express Cre recombinase under the direction of wingless-related MMTV integration site-1 (*Wnt1*) promoter/regulatory sequences therefore restricting expression to the neural tube and subsequently the neural crest cell population. The male progeny that are *Tcfap2 β* ^{+/-} / *Wnt1Cre*^{+/-} are then crossed *Tcfap2 β* ^{lox/lox} to generate conditional mutants in which the mutants are heterozygous for a *Tcfap2 β* null allele and have a disrupted *Tcfap2 β* allele due to Cre-mediate excision specific to the NCC by the loxP sites.

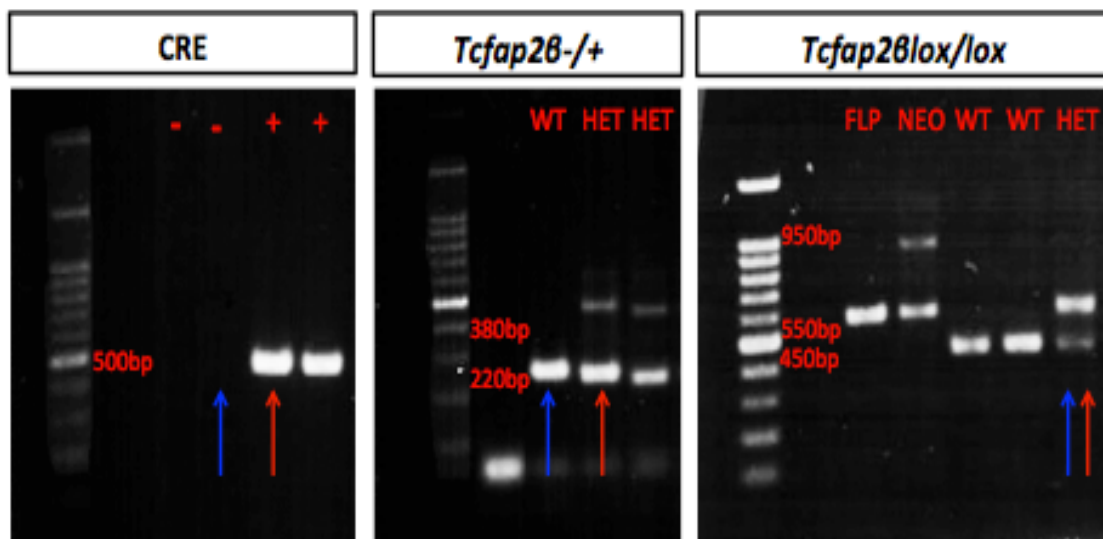


Figure 7. PCR results. Mice from the final cross that genotyped positively for the presence of Cre recombinase, heterozygous for the $Tcfap2\beta^{BKO/+}$ null allele and heterozygous for the $Tcfap2\beta^{lox}$ allele (as indicated by the red arrow) were considered to be AP-2 β NCC KO mutants. Littermates that genotyped negative for Cre recombinase, homozygous wildtype for the $Tcfap2\beta^{BKO/+}$ null allele and heterozygote for the $Tcfap2\beta^{lox}$ allele (as indicated by the blue arrow) were used as control littermates when available.

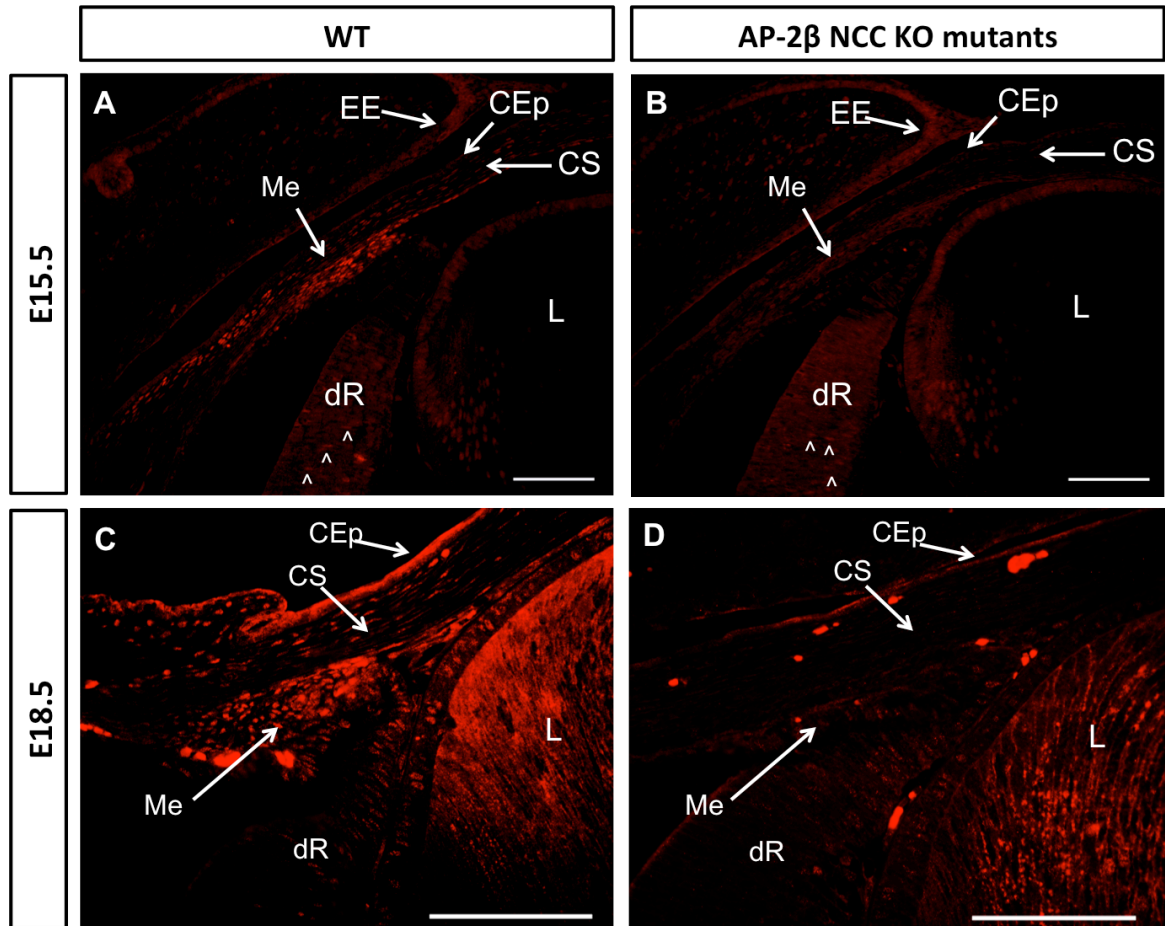


Figure 8. Conditional deletion of AP-2 β in the NCC population in AP-2 β NCC KO mutant embryos. (A) AP-2 β expression in the periocular mesenchyme (Me), the eyelid epidermis (EE), the developing corneal epithelium (CEp) and corneal stroma (CS), and developing retina (dR) (arrowheads) of the anterior eye of an E15.5 wildtype embryo (L; lens). **(B)** AP-2 β conditionally deleted in the NCC population with no expression displayed in the Me and CS, but retained in the dR (arrowheads), EE and CEp. **(C)** Expression of AP-2 β in the anterior eye of an E18.5 wildtype murine eye in the Me, CS and CEp. **(D)** AP-2 β expression deleted conditionally from the ME and CS, but retained in the CEp. Scalebars set to 100 μ m.

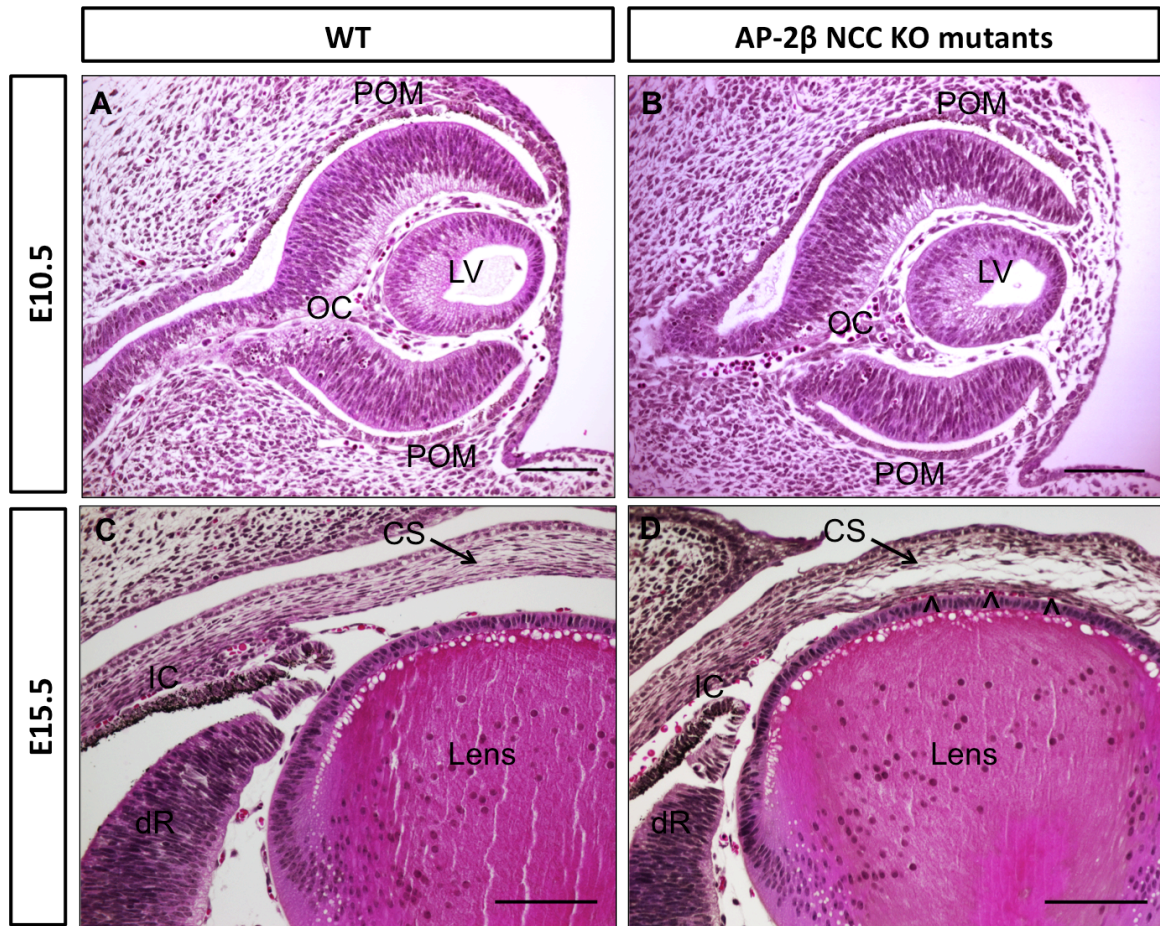


Figure 9. Early eye development of AP-2β NCC KO mutants relative to wildtype littermates. (A)(B) Histologically there appears to be no difference between mutant and wildtype eye development at E10.5. (C)(D) Mutant corneal stroma (CS) appear to be more diffuse with increased spaces between collagen fibrils and an adjacency between the cornea and lens (arrowheads), when compared to wildtype littermates at E15.5 (POM; periocular mesenchyme, OC; optic cup, LV; lens vesicle, IC; iridocorneal angle, dR; developing retina). Scalebars set to 100μm.

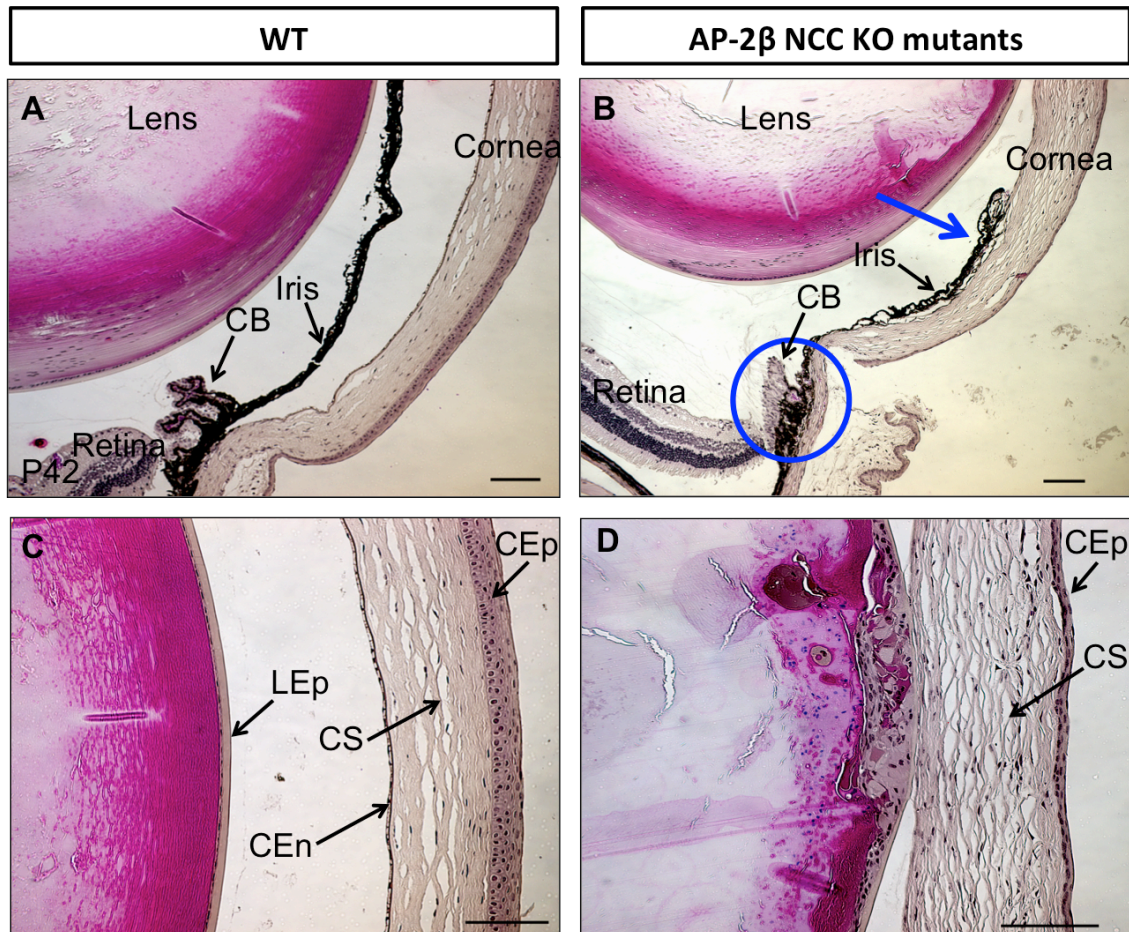


Figure 10. Abnormal development of the anterior segment in P42 AP-2 β NCC KO mutants. (A) Wildtype littermate, all structures are intact (CB; ciliary body). (B) KO mutant displayed a disrupted iridocorneal angle (blue arrow) with the iris adhered to the corneal stroma, and an atrophied ciliary body (blue circle). (C) Wildtype (LEp; lens epithelium, CEn; corneal endothelium, CS; corneal stroma, CEp; corneal epithelium). (D) KO mutant displaying a disorganized and hypercellular stroma, and reduced stratification of the corneal epithelium. Scalebars set to 100 μ m.

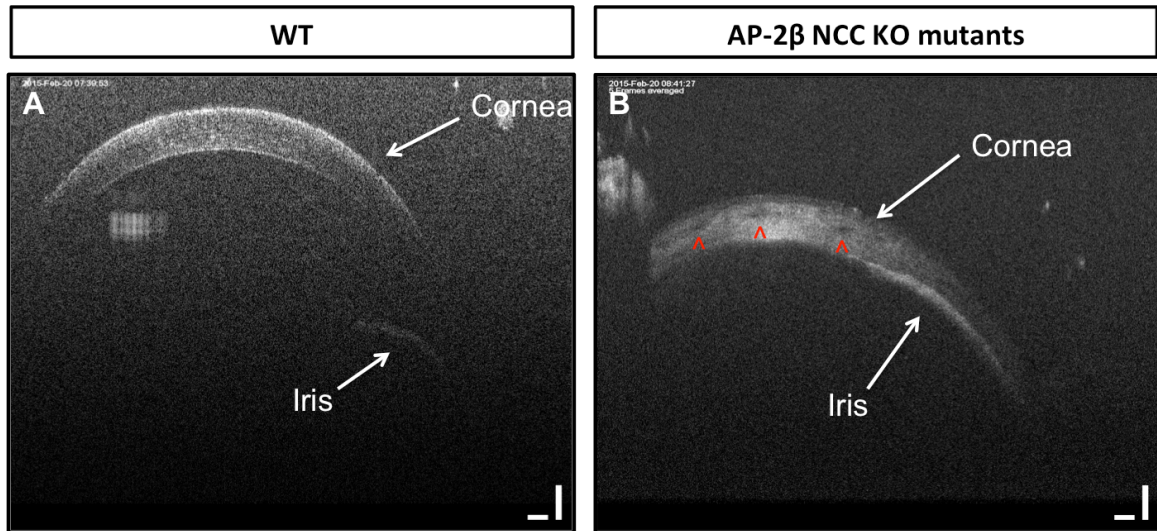


Figure 11. OCT images displaying a closed iridocorneal angle of a P42 AP-2 β NCC KO mutant. (A) An OCT image of the anterior chamber of a wildtype mouse. **(B)** An OCT image of the anterior chamber of an AP-2 β NCC KO mutant with adherence of the iris to the cornea (arrows) and the presence of round foramen in the corneal stroma (red arrowhead).

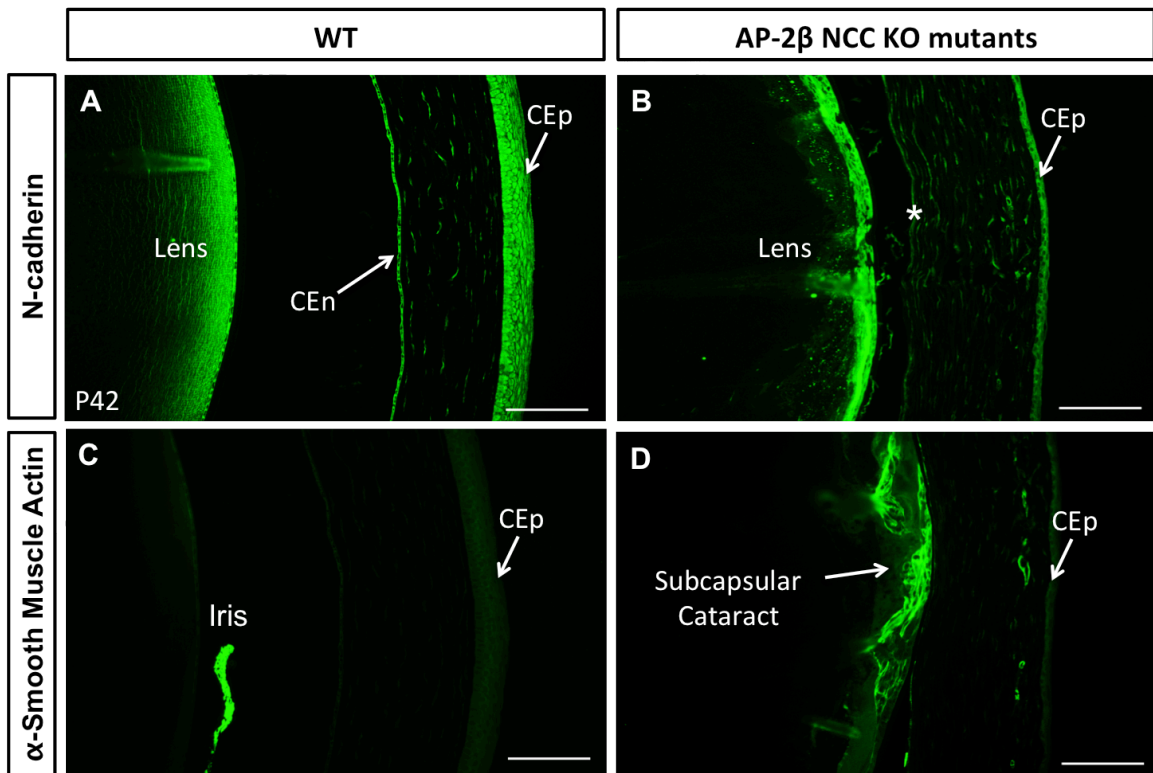


Figure 12. Missing corneal endothelium and anterior subcapsular cataracts in P42 AP-2β NCC KO mutants. (A) Wildtype N-cadherin staining of the corneal endothelium (CEn). (B) KO mutant with no staining of the corneal endothelium (*). (C) Wildtype α-smooth muscle actin staining (I; Iris). (D) KO mutant displaying an anterior subcapsular cataract, epithelial to mesenchymal transition confirmed with α-smooth muscle actin staining. Scalebars set to 100μm.

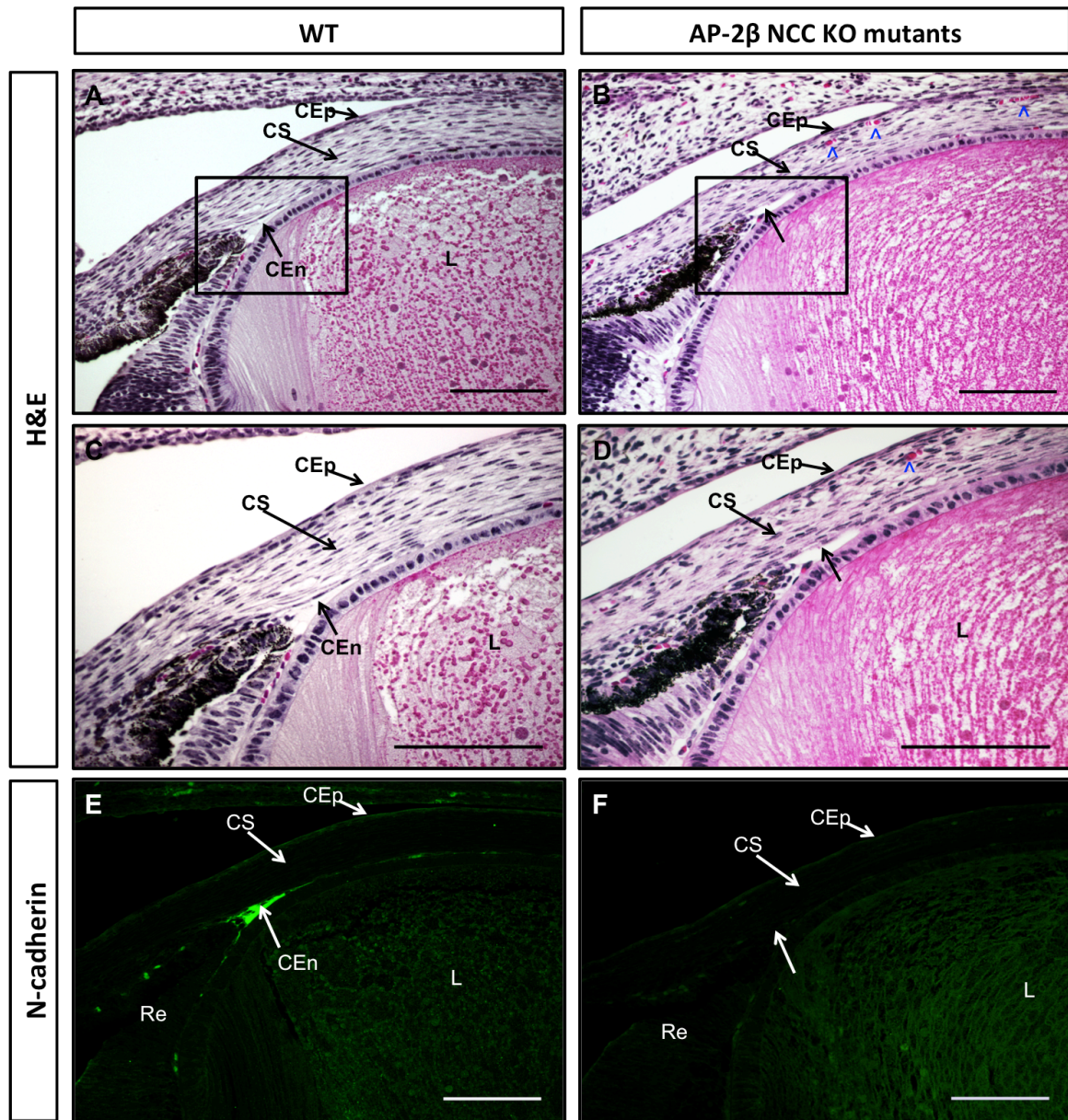


Figure 13. Missing corneal endothelium in E18.5 AP-2 β NCC KO mutant embryos. (A)(C)(E) Corneal endothelium present (arrow) in E18.5 wildtype littermates with positive N-cadherin staining of the endothelium. (B)(D)(F) No endothelial cells stained in the iridocorneal angle of E18.5 AP-2 β NCC KO mutants, confirmed with no expression of N-cadherin (arrow). Red blood cells also present in the corneal stroma (blue arrowheads) suggesting neovascularization of the cornea. Scalebars set to 100 μ m.

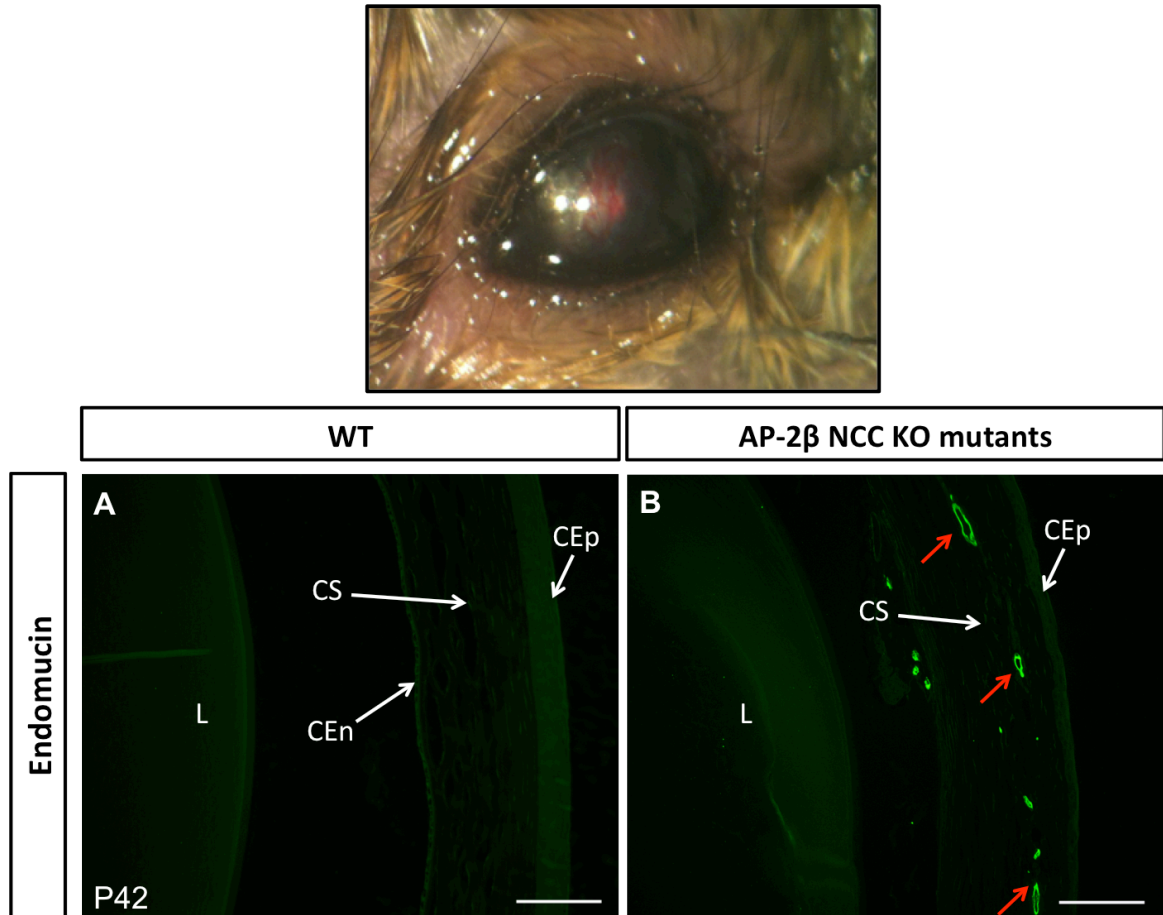


Figure 14. Corneal neovascularization in P42 AP-2 β NCC KO mutants. Red blood vessels were observed in AP-2 β NCC KO mutants. (A) No staining in the wildtype littermate corneal stroma. (B) Presence of blood vessels confirmed in the corneal stroma of the AP-2 β NCC KO mutants with positive endomucin staining (red arrows). (L; lens, CEn; corneal endothelium, CS; corneal stroma, and CEp, corneal epithelium) Scalebars set to 100 μ m.

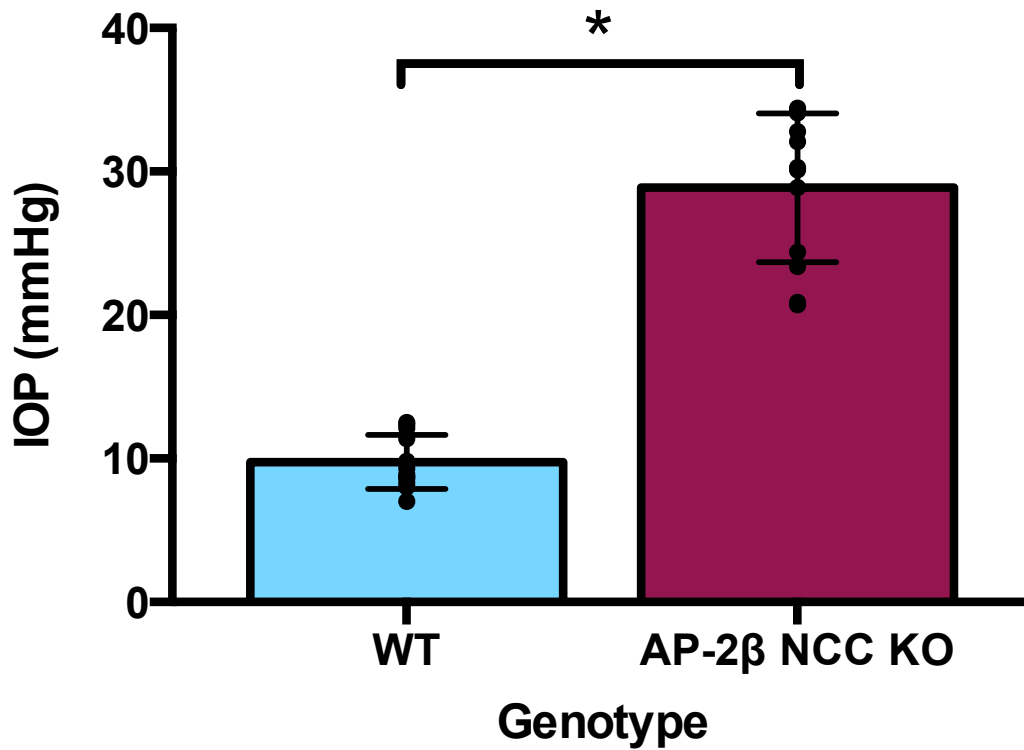


Figure 15. A comparison of intraocular pressure (IOP) between three-month-old AP-2β NCC KO mutants and their wildtype littermates. AP-2β NCC KO mutant mice have increased IOP (28.87mmHg ± 5.19, n=12) relative to their wildtype littermates (9.76mmHg ± 1.88, n=12). Measurements taken with a Rebound Tonometer (TonoLab Vantaa, Finland) (Mean ± SD; *P < 0.0001, Student's two tailed t-test).

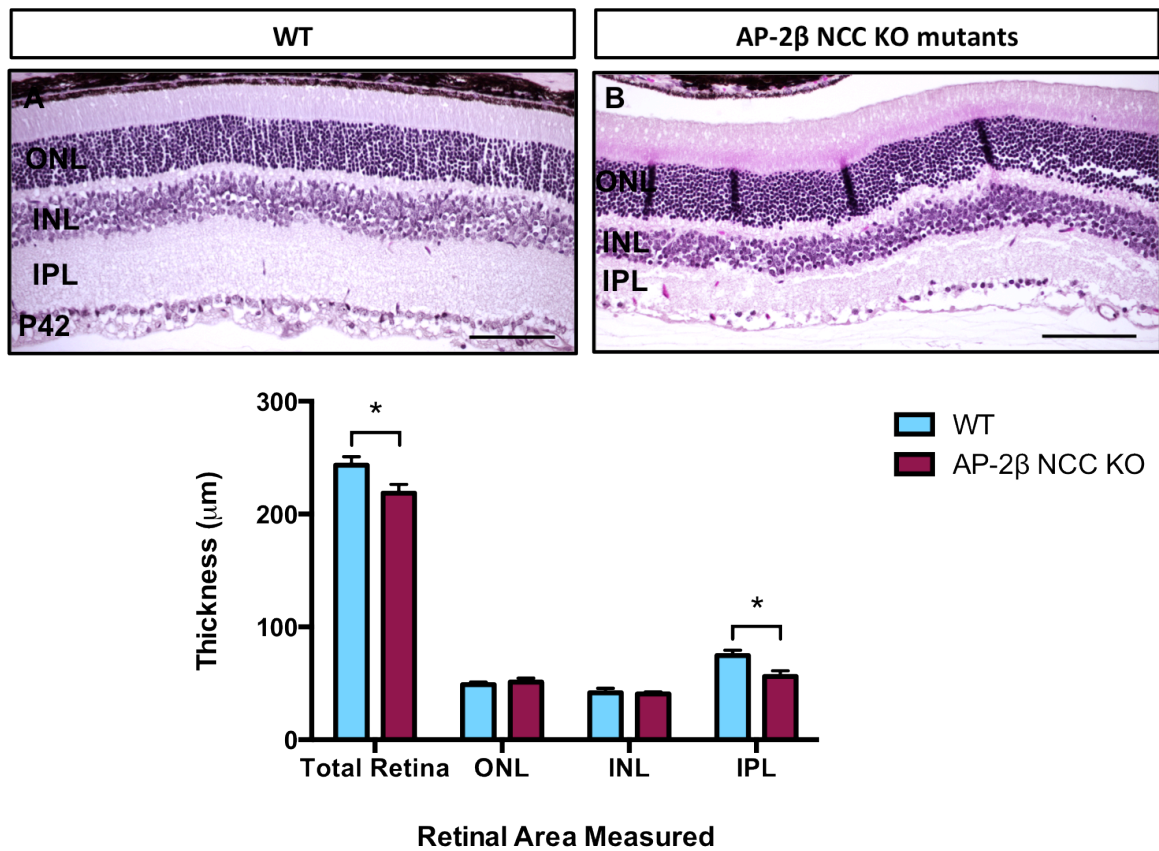


Figure 16. Decreased overall retinal and IPL thickness in P42 AP-2β NCC KO mutants. E18.5 AP-2β NCC KO mutants have a significantly decreased overall retinal thickness ($218.56\mu\text{m} \pm 7.90$, $n=4$) and a decreased inner plexiform layer (IPL) ($56.11\mu\text{m} \pm 5.00$, $n=4$) relative to their wildtype littermates ($243.47\mu\text{m} \pm 7.38$, $n=4$, and $74.67\mu\text{m} \pm 4.80$, $n=4$, respectively). There was no significant difference in thickness of the outer nuclear layer (ONL) and inner nuclear layer (INL) layers of the mutants and their littermates. (Mean \pm SD; * $P < 0.005$, Student's two tailed t-test). Scalebars set to $100\mu\text{m}$.

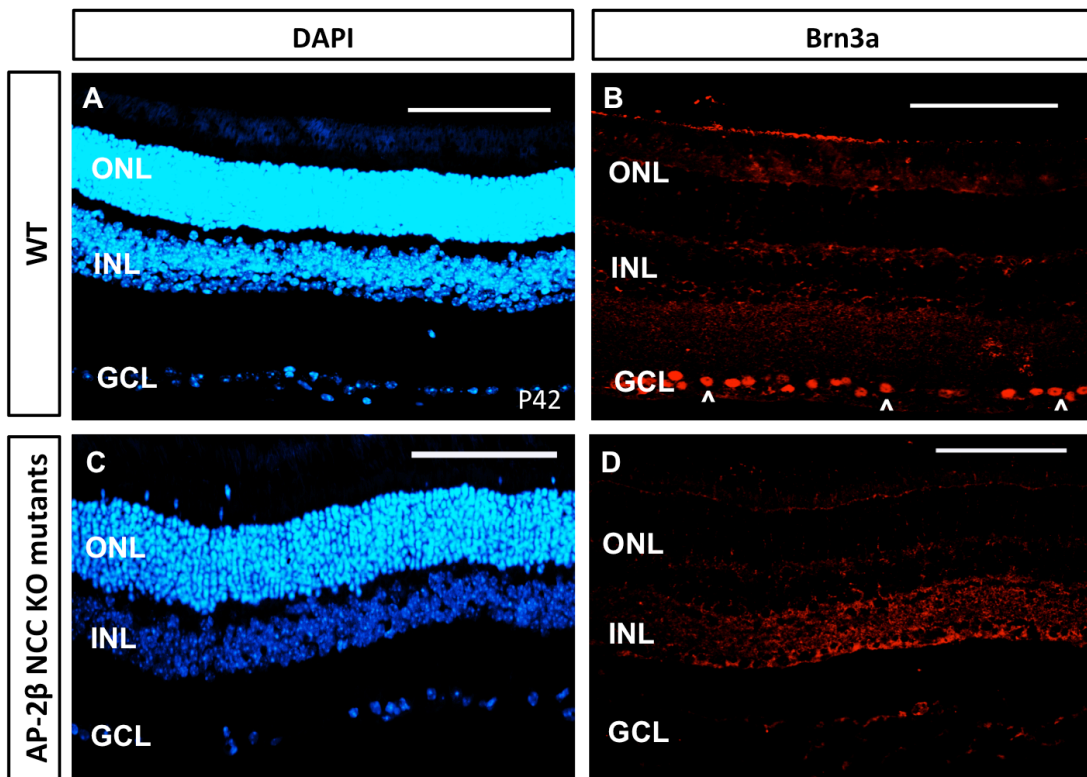


Figure 17. Loss of Brn3a expression in AP-2 β NCC KO mutants. (A)(B) Presence of RGCs in the ganglion cell layer (GCL) of P42 wildtype littermates (arrowheads). (C)(D) No expression of Brn3a, a marker of RGCs, in the GCL of the mutant retinas (n=7), suggesting the loss of RGCs (INL; inner nuclear layer, ONL; outer nuclear layer). Scalebars set to 100 μ m.

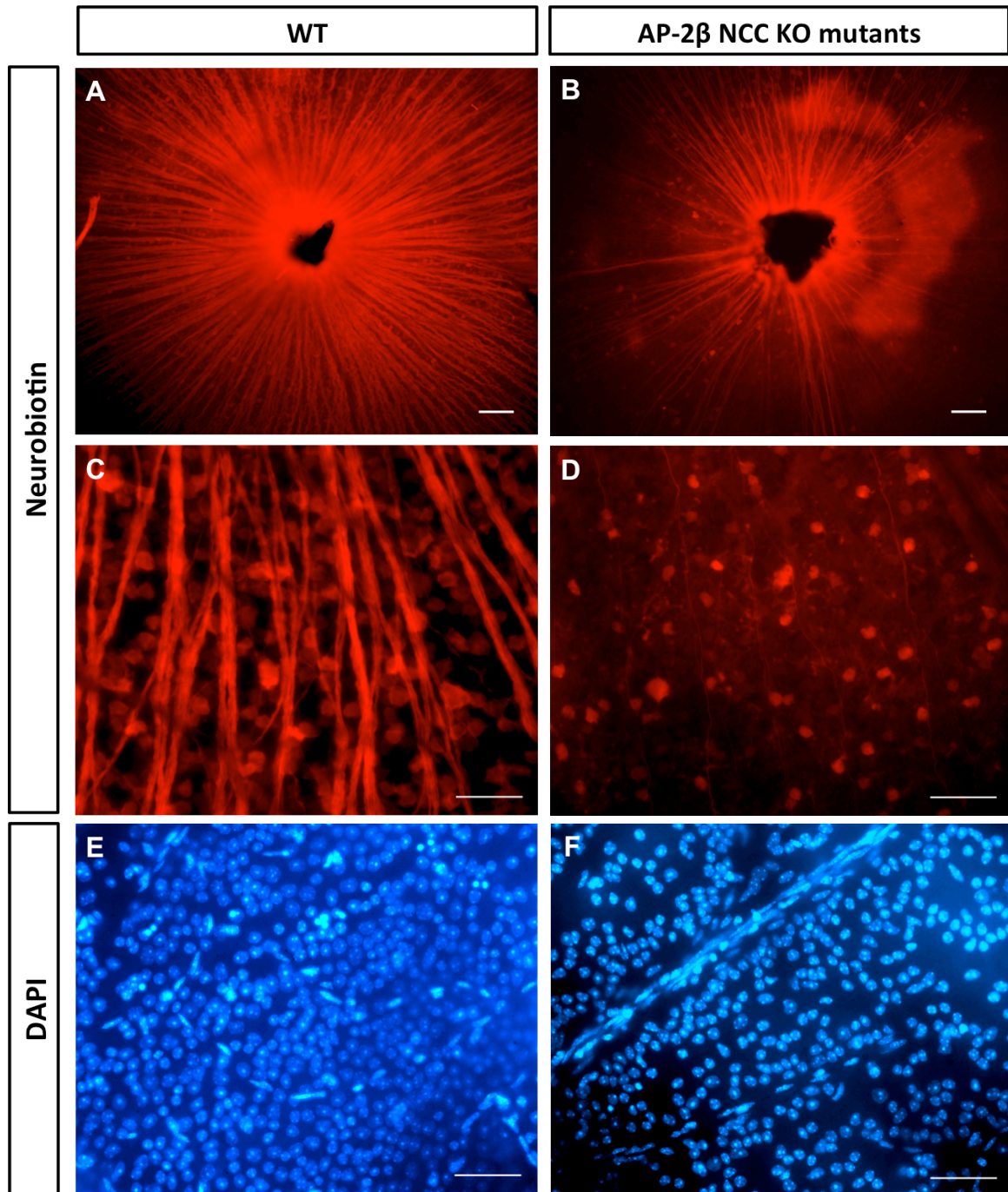


Figure 18. Labeling of RGCs and nuclei in two-month-old AP-2 β NCC KO mutants. (A)(B)(C)(D) Loss of RGC bodies and their axons in two-month-old AP-2 β NCC KO mutants when compared to their wildtype littermates. (E)(F) Decreased number of DAPI labeled nuclei in the GCL of AP-2 β NCC KO mutant retinas. Scalebars set to 100 μ m.

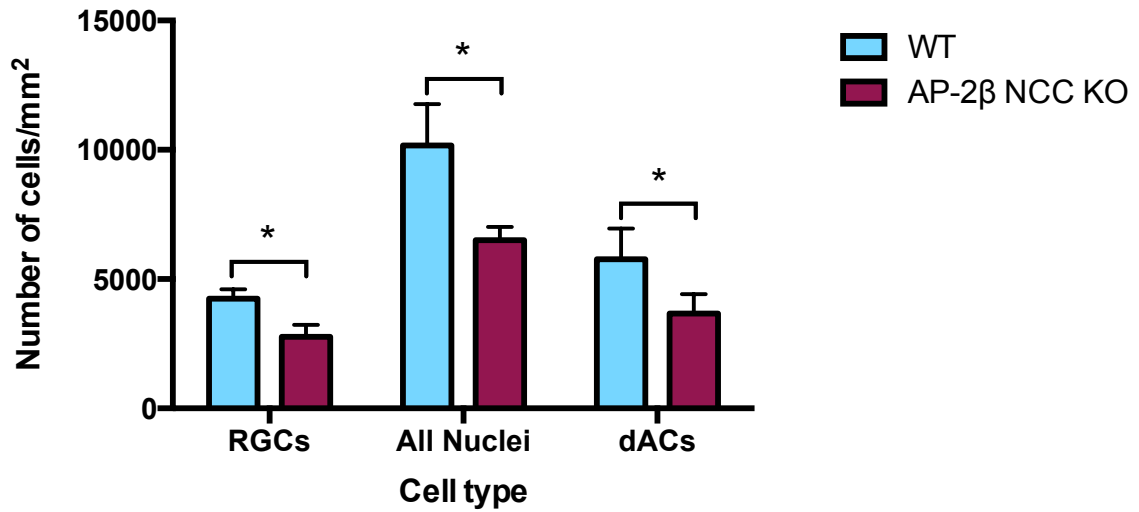


Figure 19. Decreased number of RGCs, total nuclei and dACs in two-month-old AP-2β NCC KO mutants. AP-2β NCC KO mutants have significantly decreased numbers of RGCs, total nuclei and dACs (displaced amacrine cells) per mm² (2768 ± 461, 6505 ± 511, 3663 ± 755, n=3 respectively) relative to their wildtype littermates (4244 ± 365, 10163 ± 1603, 5774 ± 1178, n=3) (Mean ± SD; *P < 0.03, Student's two tailed t-test).

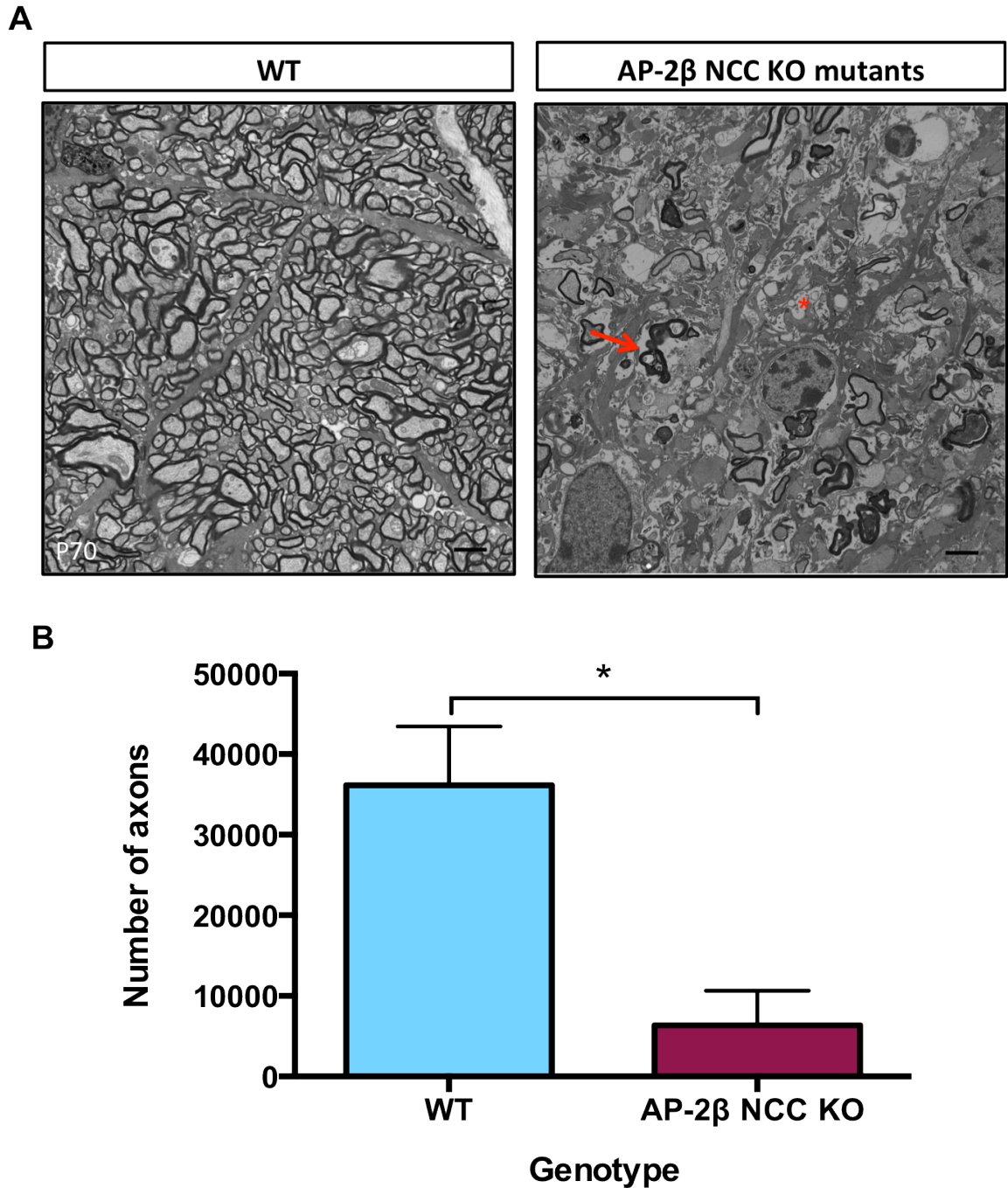


Figure 20. Transmission electron microscopy of two-month-old AP-2 β NCC KO mutant ONs and their wildtype littermates. AP-2 β NCC KO mutants display a significantly decreased number of myelinated RGC axons (6365 ± 4284 , $n=4$), degenerating axons (arrow) and areas of severe atrophy (asterisk) relative to their wildtype littermates (36143 ± 7276 , $n=4$) (Mean \pm SD; * $P < 0.001$, Student's two tailed t-test). Scalebars set to $2\mu\text{m}$.

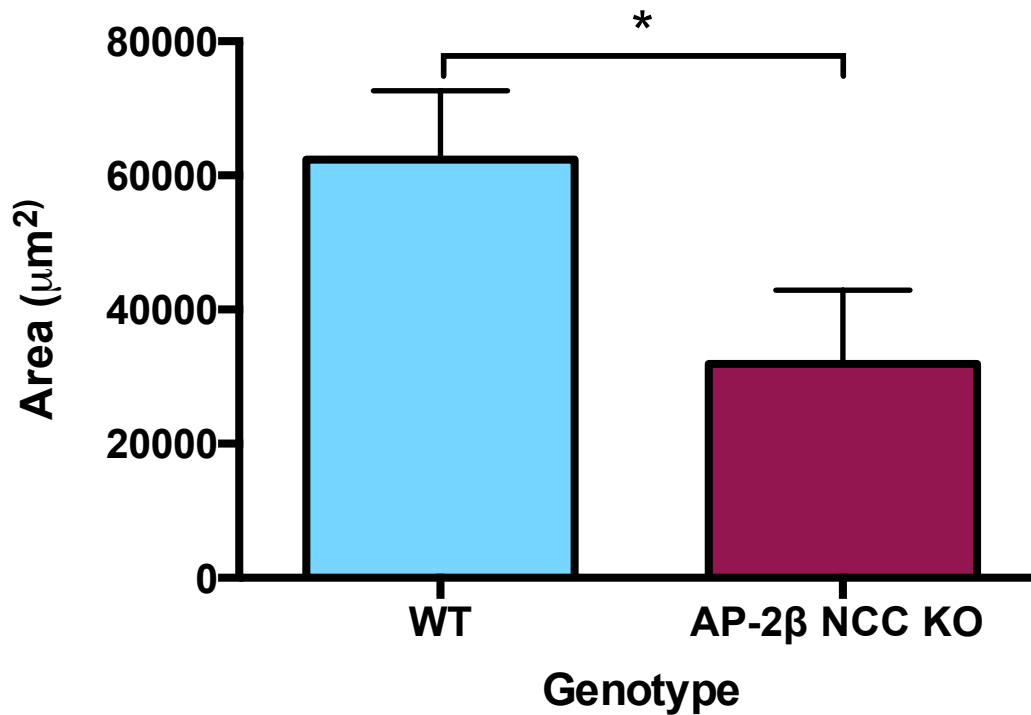


Figure 21. Decreased cross-sectional area of two-month-old AP-2β NCC KO mutant ONs. AP-2β NCC KO mutant ONs have a significantly decreased cross-sectional area ($31871\mu\text{m}^2 \pm 11016$, $n=4$) when compared to their wildtype littermates ($62286\mu\text{m}^2 \pm 10275$, $n=4$), supporting the loss of RGCs axons within the ON and the development of glaucoma (Mean \pm SD; * $P < 0.01$, Student's two tailed t-test).

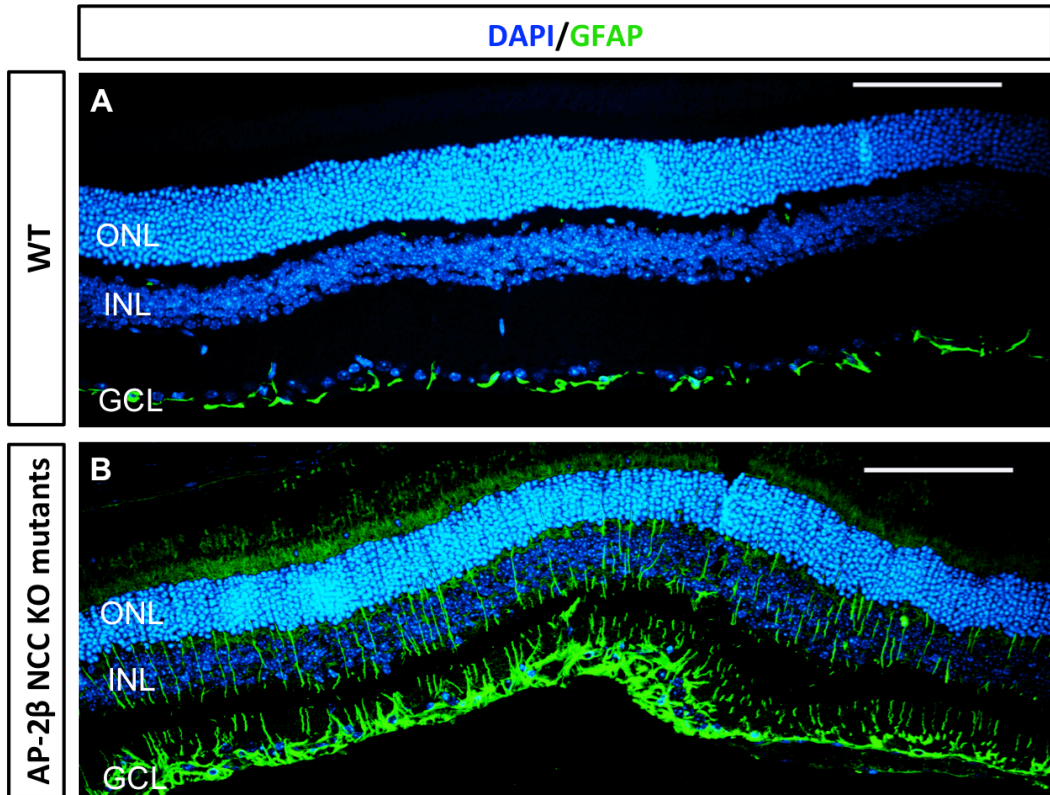


Figure 22. Increased retinal glial reactivity in the mutant retinas. Increased expression of GFAP in Müller glia cells in AP-2 β NCC KO mutant retinas supports the hypothesis of glaucomatous damage (GCL; ganglion cell layer, INL; inner nuclear layer, ONL; outer nuclear layer). Scalebars set to 100 μ m.